

Investigating the feasibility of a tool that automates the process of detecting skin cancer (malignant melanoma) using traditional computer vision techniques and the ABCDE rule.

By: Faisal ██████████ Abdul-Fattah- Student number ██████████

Abstract - Skin cancer, more specifically malignant melanoma, imposes a major health risk to people worldwide. Early detection helps increase the chances of curing the disease dramatically. This paper investigated the feasibility of strictly using computer vision and shape analysis techniques to quantify a skin lesion's features according to the ABCDE rule of melanoma. Most projects done in this domain used machine learning, an intricate field of artificial intelligence, to classify skin lesions as malignant or benign. However, no machine learning or classification was implemented for this project. This is because research has shown that machine learning can be a 'black box', meaning hard to understand and follow. Therefore, for this project, a more transparent system was produced where the final decision lies with the healthcare professionals, fostering trust in technology's use in healthcare. After pre-processing and segmenting the images, each feature was quantified according to the ABCD rule on a scale of 1-10. The number assigned to each feature was then multiplied by a specific multiplier according to the importance of the feature, providing a weighted final score out of 24. Messages were then printed out about the risk level according to the score. The results showed that the final score can successfully differentiate between malignant and benign lesions, notwithstanding expected outliers. Next, the evolution was quantified through the difference in the scores for each feature in two images taken over time as well as the total score difference which was scaled between 0-10. The software can be implemented as an application used with a mobile attached to a dermatoscope attachment.

Keywords: Melanoma detection, computer vision, image processing, 2D ABCDE feature quantification

1. INTRODUCTION

Skin cancer rates are rapidly rising around the world (Gregory and editor, 2024). Out of the three types of skin cancer, melanoma is the deadliest. Even though melanoma accounts for only 1% of the diagnosed skin cancer incidences, it leads to 75% of deaths (Ali, Li and Yang, 2020). The percentage of people diagnosed with melanoma is predicted to rise by 9% in the UK between 2023-

2025 and 2038-2040 ('Melanoma skin cancer incidence statistics', 2015). However, melanoma is highly curable if it is diagnosed early (Cleveland Clinic, 2021). Early-stage invasive melanoma has a 5-year survival rate of 94%, while for late-stage melanomas the 5-year survival rate is only 17% (Ali, Li and Yang, 2020).

The challenge is that skin abnormalities are some of the most difficult issues for a pathologist, a doctor who examines body tissue to investigate illnesses ('What Does a Pathologist Do and How To Become One? | AUC', 2021), to diagnose. Research (Jake Ellison, 2022) has shown that different pathologists who analyse the same skin abnormality can come up with clashing diagnoses. Even the same pathologist will sometimes give two strikingly contrasting diagnoses of the same case on two separate occasions. On top of that, when questioning dermatopathologists, about 50% of them thought that non-invasive melanoma is over-diagnosed, and a third thought that invasive melanoma is over-diagnosed. When a disease is over-diagnosed, this means that the disease will not hurt the patient in their expected lifetime. This is where a disastrous problem arises. Plenty of people are being tragically told that they have cancer, which leads to paying endless amounts of money for unnecessary treatment. Since this is the most serious type of skin cancer, a melanoma diagnosis can lead to devastating financial, medical, and emotional harm. Through these mistakes, the people truly suffering from the disease will get lost in the crowd of the misdiagnosed. Additionally, most of the dermatopathologists agreed that there are too many unnecessary skin biopsies and that some cases should not have been biopsied at all. These biopsies happen because of erroneous judgment that a skin lesion may be cancerous. Besides, it can be costly and time-consuming to consult a specialist to look at each skin lesion to determine whether any of them are cancerous, especially if there are a high number of lesions to be looked at. A skin cancer treatment consultation usually costs £200-£300 at a private hospital, with no health insurance ('Private Skin Cancer Cost | GoPrivate.com', n.d.). The provision of a quick

objective tool that can help GPs and doctors with decision-making can therefore reduce over-diagnosis, save time and money, and reduce the number of unnecessary skin biopsies. The goal isn't to replace doctors but rather to make their jobs easier and more successful by collaborating with an objective computer.

In the past few decades, numerous studies explored computational methods to help healthcare professionals diagnose melanoma early. (Moura *et al.*, 2018) used the ABCD rule and trained Convolutional Neural Networks (CNN), a machine learning algorithm, to classify skin lesions. (Alizadeh and Mahloojifar, 2018) produced a mobile application for melanoma detection that uses Support Vector Machines, a machine learning based classifier, to classify lesions. (Firmansyah, Kusumaningtyas and Hardiansyah, 2017) was the most similar study to this current project in that they used traditional computer vision techniques without machine learning. They used the ABCD rule and a mobile device for the software. Then, they used a criterion called the TDS score to classify lesions. Research therefore showed that most of the studies done on this topic involved machine learning or classification and neglected the evolution feature of the ABCDE rule.

The current project introduces essential novel ideas. Firstly, the quantification of the lesions is unique and easier to understand relative to conventional methods. Most research used the TDS score (Durgarao and Sudhavani, 2018) to quantify features. This current project also used the TDS criterion. However, the difference lies in the fact that usually when the TDS criterion is used, it involves having different score ranges for each feature, for example the asymmetry feature is assigned a score of 0-2 while colour 1-6, etc. For this current project, a single score range of 1-10 is assigned to each feature. This is easier and simpler to understand. Additionally, using the conventional score ranges for the features and then weighting the features gives a TDS score out of 8.9. Using the current project's score ranges gives a final score out of 24. Again, this is simpler to understand. Moreover, the project proposed a novel approach to quantify evolution which is typically neglected in research by measuring the difference in scores of the lesion over time. Furthermore, this current project involved no classification because classification means the computer is making a crucial decision rather than the healthcare professional. In the traditional

methods that use machine learning, the computer classifies the lesions, but clinicians have complained machine learning can be like a 'black box' (Patel, 2023). This means its decisions can be sometimes extremely difficult to understand. The current project proposes a more transparent system that can easily be understood by most people while keeping the final decision in the healthcare professionals' hand. It is essential to have research like this current project that attempts to add unique additions to existing research and can help make the general populace and especially healthcare workers more trusting of technology integration into healthcare. There is also novelty introduced in the methodology that will be explained in section 2.

The current project's objectives include investigating the feasibility of a tool that automates the process of analysing skin lesions and quantifying the features of the ABCDE rule, a system used by clinicians to spot melanoma ('THE "ABCDE" RULE', 2016). Moreover, investigating the motivation for the project, the physical design and market for the tool, and how it compares to other existing tools. The dataset used was the ISIC 2020 Challenge Dataset ('The ISIC 2020 Challenge Dataset', 2020)

2. METHODOLOGY

2.1. Pre-processing

Pre-processing the pictures is essential to ensure the images are clean and suitable for analysis.

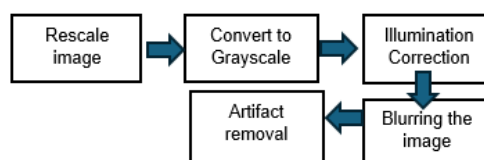


Figure 1: Pre-processing steps flow chart.

2.1a) Re-scale the image

The first step was to re-scale the images to 600x400px so there was a common dimension for all the images used for analysis leading to accurate and reliable analysis.

2.1b) Convert to Grayscale

This simplified the subsequent processing steps. Grayscale images have only one channel/intensity ('Why to use Grayscale Conversion during Image Processing?', n.d.) (see appendix 1a).

2.1c) Illumination correction

This step allowed control of the brightness of the image and hence illuminated dark images or darkened bright images (Agarwal and Patnaik, 2021)(see appendix 1b).

2.1d) Blurring the image

Gaussian blur was added. This applied a Gaussian filter, helping with noise removal.

2.1e) Artifact removal

Artifacts are undesirable changes present in images. The artifacts most prevalent in the dataset used were hair and ruler markings. (Talavera-Martinez, Bibiloni and Gonzalez-Hidalgo, 2021) compared six of the best methods of hair removal. From the results, one of the best performing methods was the DullRazor method. The process entails applying a sequence of morphological operations to the image so that a mask is produced that holds the hairs (Velasquez, 2022) (appendix 1c). However, a notable limitation with computer vision methods of hair removal is that valuable information can be lost from the lesions (appendix 1e). Consequently, for some of the analysis carried out through this project, if there was hair on the lesion itself, and removing it altered the characteristics of the lesion, the hair was kept there. If removing the hair did not omit essential details, it was removed. An alternative method to remove hair applied through this project involved contour filtering. This can also remove ruler markings. This is explained in step 2.2c.

2.2. Segmenting the lesion methodology

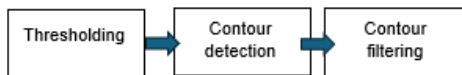


Figure 2: Segmenting the lesion steps flow chart.

2.2a) Thresholding

There are many thresholding techniques, however the commonly used one for medical image processing purposes is called Otsu Thresholding (baeldung, 2023). This method constitutes separating an image into two classes, the background and foreground, based on the intensity of pixels on the grayscale. This partly segments the image i.e. separates the lesion and the surrounding skin. However, this was still not ideal at this point as can be seen in appendix 1f. There are black blobs near the corners of the image, when the entire background should be white.

2.2b) Contour detection

All the contours/outlines from appendix 1f are detected including for the unwanted blobs.

2.2c) Contour filtering

This is done by a loop in the code which iterates through each of the contours detected on the image and then filters the smaller contours or noise regions detected. Only a contour with an

area of over 150,000 pixels (the contour around the lesion itself) was taken for the current project. This ignored the smaller contours that were drawn around rule markings, hairs, random blobs, etc.



Figure 3: Image after pre-processing and segmenting.

3. QUANTIFYING THE FEATURES

3.1 Asymmetry

The first of the ABCDE rules is Asymmetry. If a skin lesion is asymmetrical, where one half does not match the other, this may indicate that it is cancerous (Pietrangelo, 2022).

The first method of measuring asymmetry attempted through this project drew inspiration from the SIFT (Scale-Invariant Feature Transform) method that (Ali, Li and O'Shea, 2020) executed. This is a computer vision technique initially identifies distinctive key features in an image. Subsequently, it matches these key features to the key features of a different image of the same shape (Singh, 2019). In the case of the current project, the key features of the right and left half of the lesion, and top and bottom half, were matched. This technique offered advantages like not being affected by the size or orientation of the image. This meant that images did not need to be rescaled at the start. However, the reason it was not picked was because SIFT is heavily affected by blur (Sult et al., 2021) (appendix 2b). Therefore, a different solution had to be explored. (Sabouri, 2016) and (Garnavi, Aldeen and Bailey, 2012) mentioned a variable called the circularity index that can be calculated to quantify asymmetry. This measures how closely a shape resembles a circle, which is an infinitely symmetrical shape. A circularity of 1 means infinitely symmetrical, which is the circularity index of a circle. The lower the circularity index and the closer it gets to 0, the more asymmetrical. The formula for this is as shown in Equation 1

$$\text{Circularity} = \frac{4\pi A}{P^2} \quad (1),$$

where A is the area and P is the perimeter. First, a contour/outline was drawn around the region of interest, which was the skin lesion, so that the area and perimeter could be computed using computer vision functions. After that, the circularity was computed (See appendices 2c-2l).

The current project also tested a third method to quantify asymmetry which was a novel

approach relative to typical melanoma papers. (D.J.Dunn, n.d.) mentioned how for symmetrical shapes, the centroid of the shape, which is the centre of the shape, is perfectly halfway between the top and bottom/right and left edges, while it isn't for asymmetrical shapes. Therefore, the centroid of the skin lesion needed to be found to advance with this method. In terms of computer vision, the centroid can be thought of as the weighted mean of all pixels making up a shape (Bapat, 2018). To do that computationally, Image Moments were used. Image Moments can be defined as specific weighted means of an image's pixel intensities. To find the centroid, the equations 2 and 3 were used. Equation 2 finds the x coordinate of the centroid while equation 3 finds the y coordinate. M represents the Moment.

$$C_x = \frac{M_{10}}{M_{00}} \quad (2)$$

$$C_y = \frac{M_{01}}{M_{00}} \quad (3)$$

After computing the centroid, two points on the border of the lesion directly to the right and left sides of the centroid were found. Same with directly above and below the centroid. Then the distances from the centroid to each of these four points was found (radius). Then the difference between the top and bottom radius was computed. Same with the left and right radii. The differences were added to get a total difference. The higher this total, the more asymmetrical the shape (appendices 2m-2v).

Both the circularity index and the centroid method were flawed in that they are less detailed relative to methods employed in other papers, such as the aforementioned SIFT method. However, the simplicity of circularity and centroid methods was also an advantage. Simply, a centre point is found, and radii are compared, while for circularity the shapes are compared to a circle. If the complexity of traditional methods has deterred clinicians before, then simplification is essential. The clinicians do not need to understand every single step of quantifying the features but having a basic understanding of the methodology can help build confidence and trust in this system. Knowing how it was quantified and understanding the rationale behind the numbers is crucial to facilitate the use of these in healthcare. It is also easier to check the validity of the results if they understand the methodology in some way as they can spot if a result is way out of its expected range.

Therefore, the circularity and centroid methods were used together. To combine both

methods, the value of the total radii difference was divided by the the circularity index to give a value of the asymmetry index (A). The more asymmetrical, the higher the value of A is. The range of values of A was wide and hence difficult to understand. So, the values of A were scaled between 1-10 for ease of understanding. The ranges were as shown below.

1 if $0 < A \leq 1$, 2 if $1 < A \leq 3$, 3 if $3 < A \leq 6$, 4 if $6 < A \leq 9$, 5 if $9 < A \leq 12$, 6 if $12 < A \leq 15$, 7 if $15 < A \leq 18$, 8 if $18 < A \leq 21$, 9 if $21 < A \leq 24$, 10 if $24 < A$

These specific ranges were chosen by testing many images, malignant and benign, and identifying what the typical value of A was for malignant and benign lesions. Typically, for obviously malignant the value of A was over 18, and for obviously benign the value was lower than 6. Note that if the value of the numerator of the formula for A was 0, i.e. the total difference was 0, then the circularity was taken to be equal to A. This maintained the pattern of more asymmetrical meaning a lower value of A.



Figure 4: Asymmetry index (3) of a malignant lesion.

3.2 Border irregularity

The next feature was Border irregularity. Cancerous skin lesions have irregular, ragged or blurred edges ('Signs of Melanoma Skin Cancer | Symptoms of Melanoma', 2023).

(Do et al., 2018) mentioned that convexity is a shape feature that can be used to measure border irregularity. Convexity is how a shape's contour differs from a smooth convex outline. (Deci Team, 2023). The simplest convex shape of a shape is called its convex hull. Therefore, to measure the border irregularity, the process entailed drawing the convex hull around the shape, and then finding the difference between the convex hull and the actual contour of the shape. This difference is called the convex defect (Pandey, 2021). To quantify this, a convexity ratio was calculated (appendix 3a):

Convexity ratio=shape's actual contour (4) perimeter/convexity hull perimeter

Irregular shaped should have higher values of the convexity ratio. This shape feature was advantageous as the convexity ratio was invariant to similarity transformations such as rescaling,

meaning the images did not need to be rescaled at the start. However, this method was not picked due to its computational complexity (Jovišažunić and Rosin, n.d.). This project was done on a laptop and no hardships were faced due to the computational complexity, but the aim of this project is to be implemented on a less powerful smaller smartphone and so a method like this would be too intensive. The speed of the results for a healthcare project like the current one are important and the speed will be slower for more computationally complex algorithms.

The next method tested was calculating a value called the compactness (Do et al., 2014). There are various ways to calculate compactness. The method attempted through this paper was by a measure called the Reock Score ('Geometry and Compactness', n.d.).

$$R = \frac{\text{Area of district}}{\text{Area of the smallest square containing the district}} \quad (5)$$

The issue with this metric is that the difference in values was not apparent between the malignant and benign lesions (appendices 3b-3k). Therefore, a third measure called irregularity index (She, Liu and Damatoa, 2007) was used (appendices 3l-3u). This was less computationally complex and yielded more obvious differences in the results between the malignant and benign lesions. The formula for this is shown in formula six.

$$I = \frac{P^2}{4\pi A} \quad (6)$$

Then to scale "I" between 1-10 the following ranges were picked after rigorous testing.

1 if $I=1$, 2 if $1 < I < 1.05$, 3 if $1.05 < I < 1.1$, 4 if $1.1 < I < 1.15$, 5 if $1.15 < I < 1.2$, 6 if $1.2 < I < 1.25$, 7 if $1.25 < I < 1.3$, 8 if $1.3 < I < 1.35$, 9 if $1.35 < I < 1.4$, 10 if $I > 1.4$



Figure 5: Border irregularity index (4) of a benign lesion.

3.3 Colour variegation

Benign lesions typically are a single shade of brown and are uniformly coloured. Malignant ones have differing colours and may contain shades of brown, tan or black, or even areas of red, blue, or white (Ann Pietrangelo, 2022).

The first step of testing this method involved taking the segmented binary image from figure 3 and then imposing the actual-coloured

lesion on top of the white pixels (appendix 4a). After this step, the colour variegation of the lesions could be tested.

The first method explored involved the implementation of a technique called colour masking (Riswanto, 2023). Colour masking turns an image into a binary form by specifying particular colour ranges. Through these colour ranges, one can isolate specific shapes and objects within the image that consist of these colours. To initiate this process, the colour format was converted from RGB to HSV because it is more suitable for colour-based segmentation (Fernando, n.d.). Next, upper and lower thresholds were defined for six of the colours sometimes found in malignant lesions- white, dark brown, light brown, blue, black, and red. After that, a binary colour mask was applied on the image from appendix 4a where the pixels within the specified colour range were set to white (255) and pixels outside the range were set to black (0). Subsequently, conditional statements were used that verify whether the colour masks for each colour had pixels with a value of 255 (white), hence confirming the presence of that specific colour. If there was, then a message was printed out saying for example: "Red: 1". If there was no colour detected and the pixels were all black, then "Red: 0". However, this method presented a few problems when used alone. The first was the fact that the specified ranges for the colours were not perfect. Although rare, there were some cases where there was a shade of a colour present in the lesion that was outside the range specified. Furthermore, there was the problem with detecting the colour black. The mask shown in appendix 4a has a background of black. Therefore, the system was always going to output "1" for black because it was in the background. Therefore, code was written that checks if imposing the coloured lesion adds black pixels to the image (appendices 4i-4l). This method was beneficial in that it was easy to understand for doctors. Therefore, after fixing the issue with detecting the colour black, the method was still used. But, to increase the reliability of the data, the following two methods were combined with it.

A paper by (Hasler and Suessstrunk, 2003) analysed a factor called 'colourfulness'. According to research, this was not usually used for melanoma detection. However, as a novel approach, this paper investigated the possibility of using colourfulness to quantify colour of skin lesions as it can provide a measure of the

variation/uniformness of the colours in a skin lesion. To do this computationally, first the colour space needed to be converted to RGB since an image needs to be in RGB format to calculate colourfulness. The opponent colour representation then needs to be found (Rosebrock, 2017). To do this, equations 7 and 8 were used. R represents red, G green, and B blue. Equation 7 shows rg which is the variance between the red channel and the green channel. Equation 8 shows yb which is half of the total of the green and red channels and then subtracted by the blue channel.

$$rg = R-G \quad (7)$$

$$yb = \frac{1}{2}(R+G)-B \quad (8)$$

After that, the standard deviation (equation 9) and the mean (equation 10) can be calculated.

Subsequently, the final colourfulness metric can be found (equation 11).

$$\sigma_{rgyb} = \sqrt{\sigma_{rg}^2 + \sigma_{yb}^2} \quad (9)$$

$$\mu_{rgyb} = \sqrt{\mu_{rg}^2 + \mu_{yb}^2} \quad (10)$$

$$\text{Colourfulness} = \sigma_{rgyb} + 0.3 * \mu_{rgyb} \quad (11)$$

The third method involved counting the number of unique colours in the lesion to measure colour variation/uniformness, inspired by (Palus, 2006). Again, this is a novel approach for melanoma research. The process was influenced by (rizvi, 2023). First the image was flattened which reshaped it into a two-dimensional array where each row represented a pixel. Each row contained three columns for each colour channel. Then the length of this set of rows and columns gave the number of unique colours in the image.

Using these three different methods added computational complexity. However, measuring colour was the most demanding feature and so an exception was made. Having three methods was necessary to ensure the colour analysis was accurate. A final value that adds the colourfulness, number of unique colours, as well as the number of the six specified colours detected was computed. However, when this calculation was made, since the scale of the colourfulness and number of unique colours number was in the thousands, the binary value for the presence of the six colours was multiplied by a thousand as well. Equation 12 shows this.

$$C = (\text{Light brown value (1/0)} * 1000) + (\text{Dark brown value (1/0)} * 1000) + (\text{white value (1/0)}$$

$$*1000) + (\text{Red value (1/0)} * 1000) + (\text{Black value (1/0)} * 1000) + (\text{Blue value (1/0)} * 1000) + \text{colourfulness} + \text{number of unique numbers}$$

(12)

Then to scale "C" between 1-10 the following ranges were used after rigorous testing.

1 if C<5000, 2 if 5000<C<6500, 3 if 6500<C<8000, 4 if 8000<C<9500, 5 if 9500<C<11000, 6 if 11000<C<12500, 7 if 12500<C<14000, 8 if 14000<C<15500, 9 if 15500<C<17000, 10 if 17000<C



Figure 6: Colour variegation index (9) of malignant lesion.

3.4. Diameter

Benign moles are typically smaller than malignant ones. If a lesion has a diameter of 6mm then that should be a sign to get it checked (Ann Pietrangelo, 2022).

Diameter of a lesion is measured as the maximum diameter between two points of the lesion outline (Mahammed et al., 2014). There are different ways of doing this including a factor called Ferret's Diameter. (Ali, Li and O'Shea, 2020) used the maximum Feret diameter which is the distance between the two farthest points on the shape's contour measured in a specified direction. However, for this current project a method utilising the diameter of a minimum enclosing circle was used instead, which is the smallest circle that completely encompasses a shape. Feret's diameter has its advantages, like its alignment with the actual physical diameter of the object. Essentially, it mirrors the length that would be measured if the object were grasped between a calliper. However, the minimum enclosing circle was picked for various reasons. It is simpler to understand, and less computationally complex. (Ali, Li and O'Shea, 2020) also mentioned how Feret's diameter uses a specified direction (angle) for measurement, unlike the minimum enclosing circle. This means if the image is taken at a different angle, the diameter value may change.

After drawing the minimum enclosing circle and printing out the diameter, this value was in pixels. This needed to be converted to mm so that the lesion can be judged as having more or

less than 6mm. Converting to mm involved a process called spatial calibration (Ali, Li and O'Shea, 2020). The way this is done is through calibrating the uncalibrated image from the dataset, in pixels, against an established value, in this case mm. For the current project, this can be done if the person knew the diameter of the lesion in mm in real life which would mean a pixels/mm factor could be found. However, for most datasets including the one used in the current project, this data is unavailable. However, the dataset has most of its pictures with ruler markings displayed next to the lesion. (Ali, Li and O'Shea, 2020) calibrated their images using a single image with ruler markings on it and calibrating it. They measured that for their test images, which were 256x256px, they established a 29.7px/mm conversion factor. They used this conversion factor for the rest of their test images.

They achieved a good degree of accuracy with their method. However, with this project, a different method was used to calibrate the images. The method (Ali, Li and O'Shea, 2020) used was flawed. Using a common conversion factor for all images is prone to errors. This is because images have differing camera distances, lens focal lengths, and resolutions among other factors. In fact, tests were carried out to test their methods. Twenty images from the ISIC 2020 dataset with the same dimensions (6000x4000px) and ruler markings were taken at random. Through the application 'Paint', lines were drawn between the ruler mm markings. After that, the length in pixels of the line was divided by the number of mm to get the px/mm conversion factor. For example, for the picture in appendix 5a, the dimensions of the 5mm line drawn were 56x1332px. To get the length of the line, Pythagoras Theorem was used.
 $x=\sqrt{56^2 + 1332^2}=1333.1767\text{px}$. That represents 5mm in the ruler markings. Therefore, the conversion factor was $1333.1767/5=266.6\text{px/mm}$. This was done for twenty other images. The results are shown in appendix 5b. As can be seen from the results, even though these images were part of the same dataset, with the same dimensions, the conversion scale in some cases varied by a little bit and in some cases by a lot. So, it is not accurate to just take one conversion scale and just apply it to all images. Instead, a different novel approach was taken.

Only images with ruler markings were used. This limited the images that can be used for this tool, but the results were more accurate. A specific conversion factor was measured for each

image. The way this was done was through a new novel technique through the software that actively involves the user. All the user needs to do is manually draw a perpendicular line between two ruler consequent ruler markings (i.e. a length of 1mm). Subsequently, the programme uses the number of pixels in that line to then get a conversion factor in px/mm. Then the diameter from the minimum enclosing circle is calibrated using this conversion factor to get the diameter in mm. This method worked very well. Actively involving the users through an interactive system, especially when the users are healthcare professionals, means they are more likely to be tolerant to using the tool. The diameter was scaled to 1-10 like this:

1 if $0\text{mm} < D < 1\text{mm}$, 2 if $1\text{mm} < D < 2\text{mm}$, 3 if $2\text{mm} < D < 3\text{mm}$, 4 if $3\text{mm} < D < 4\text{mm}$, 5 if $4\text{mm} < D < 5\text{mm}$, 6 if $5\text{mm} < D < 6\text{mm}$, 7 if $6\text{mm} < D < 7\text{mm}$, 8 if $7\text{mm} < D < 8\text{mm}$, 9 if $8\text{mm} < D < 9\text{mm}$, 10 if $9\text{mm} < D$



Figure 7: Diameter size index (10) of a malignant lesion

3.5. Combining the ABCD features

It was important to then combine the results obtained to get a single output so that the results were easier to understand and interpret. There remained one more step. The features needed to be weighted according to importance of the features. To do that, the weight factors from a criterion called the TDS criterion were used. TDS only uses ABCD features and not the evolution. The evolution feature is usually neglected in research endeavours employing computers to aid melanoma detection. Often the user only wants to see the quantified total score for a single image of a lesion, excluding the evolution. Nevertheless, this project quantified evolution using a different novel approach (see section 3.6). Through the TDS criterion the score for each feature is multiplied by a multiplier.

$$\text{TDS} = [(A \text{ score} \times 1.3) + (B \text{ score} \times 0.1) + (C \text{ score} \times 0.5) + (D \text{ score} \times 0.5)] \quad (12)$$

Maximum possible total score for this project was:

$$\text{TDS} = [(10 \times 1.3) + (10 \times 0.1) + (10 \times 0.5) + (10 \times 0.5)] = 24.$$

If the total was over 12, a message of “High risk-alert a specialist” was printed out. If the total was between 8 and 12, then “Moderate risk-monitor closely” was printed out. If the total was less than 8, then “Low risk-less monitoring needed” was printed out. These numbers were discerned through careful testing.

4. RESULT EXCLUDING EVOLUTION

For the testing of the final system, a dataset of 15 images was extracted from the main data set. A small number of lesions were tested because this was just a proof-of-concept study, and it meant focus can be placed on getting every image perfectly segmented and quantified. These 15 images were carefully picked to include obviously benign, obviously malignant, deceptively benign, and deceptively malignant lesions (outliers) so that the system can be tested comprehensively. The full 15 can be seen in appendices 7a-7o.

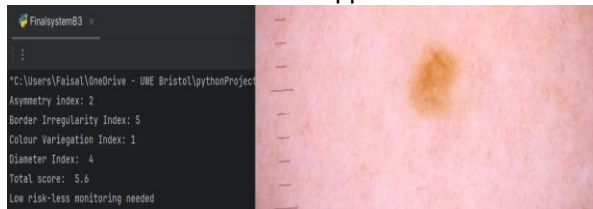


Figure 8: Final result (5.6) for a benign lesion.

5. RESULT INCLUDING EVOLUTION

The first attempt to quantify evolution was by calculating the percentage of changed pixels in the before and after pictures by computing the absolute difference between the images as seen in appendices 6a-6b. However, it was hard to understand what feature caused this change in pixels. Instead, for the software produced through this project, there will be an option on the application explained in section 6 enabling the user to save images of the skin lesions, the quantified results of the images, and the date the images were taken. Later, another image can be taken, and the difference can be quantified. This shows if the lesion evolved negatively and shows what feature of the ABCD rule became worse over time, allowing for better analysis. The dataset used for this project did not show images of lesions before and after they have evolved. Images that did in other sources online did not have ruler markings on them. So, as an innovative approach, the current project took the malignant ‘medium risk’ outlier lesion from the dataset and using a single colour the lesion was made to look more asymmetrical, irregular, more colourful, and bigger. The difference between them was quantified (appendix 6c). The evolved lesion was

classified as high risk. The difference in total score was scaled between 1-10 for clarity:

1 if $T=0$, 2 if $0 < T < 0.75$, 3 if $0.75 < T < 1.5$, 4 if $1.5 < T < 2.25$, 5 if $2.25 < T < 3$, 6 if $3 < T < 3.75$, 7 if $3.75 < T < 4.5$, 8 if $4.5 < T < 5.25$, 9 if $5.25 < T < 6$, 10 if $T > 6$

6. DEVICE WORKING SPECIFICATION

The software proposed could be implemented in the form of an application available to be downloaded on every computer worldwide, including smartphones. Some previous solutions like SkinVision and MoleScope (GentleCure, 2021) used just the app and the phone cameras for analysis. However, images from the phone cameras will be affected by glare, and not in the quality suitable for analysis. Therefore, for this paper, a smartphone compatible dermatoscope tool is proposed to be used in tandem with the application. The dermatoscope allows the phone to take clearer, and if needed, magnified images.

The device has several use cases. Firstly, a General Practitioner can use the tool to help them decide whether the skin lesions are serious enough to refer to a specialist. Secondly, self-examinations can be carried out by the general populace from home. There could be a feature where the images can then be sent to a dermatologist to get their opinion with additional costs. The costs can vary depending on how fast the response from the dermatologist is (Curtis, 2016). Moreover, the specialists and dermatologists themselves can use this tool to aid them if they are unsure about their judgements.

The aim is for the tool to be available worldwide, but the main markets would be countries like Australia, New Zealand, and Denmark who had the top three highest incidences of Melanoma in 2020 ('Skin cancer statistics | World Cancer Research Fund International', n.d.).

Research like (*Dermatoscope Comparison.*, n.d.) and (*'DermLite HÜD 2 | Smartphone Home Dermatoscope'*, n.d.) were used as a reference for the features picked and look of the tool (figure 9). Dimensions would be small and compact, about 60mmx60mmx30mm like the Hud 2 which served as the inspiration for the look. The device should not weigh heavier than 50g. The Hud 2 for example which looks similar is 38.5g. Any size of lesion can be analysed, with a maximum magnification of 10x. The cost of the Hud 2 is around 150 pounds. This proposed tool has similar features to the Hud 2,

but some extra features were added so around 170 pounds is suitable.

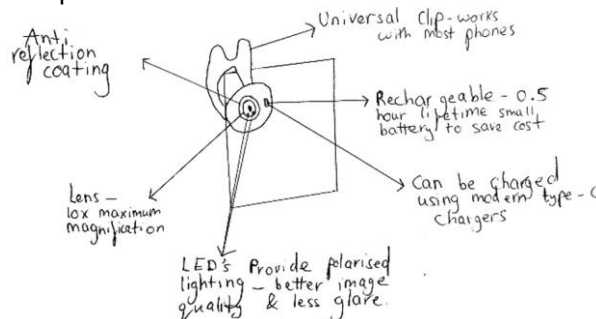


Figure 9: Design of tool.

7. DISCUSSION

The obviously malignant and obviously benign lesions were all given the correct risk level (appendix 7). However, the two outliers picked were given medium risk. This is because they had atypical features. For example, for the first outlier in appendix 8a, the lesion is benign, but the borders were jagged at certain points and quite hard to define. The diameter of the lesion was 10mm and it had a high number of unique colours too. This is why the programme placed it at medium risk. This is not a problem with the system but rather expected; there are always exceptions that defy the typical adhesion to the ABCD rule. In fact, it is a positive of the current programme that it did not place either outlier at the opposite risk level, but at medium risk. At medium risk, the user will be advised to monitor it closely. Additionally, the individual scores for each feature also behaved as expected. The table on appendix 9 shows that the malignant lesions have higher average scores for each feature. The feature that showed the highest difference between the average of the scores for benign and malignant lesions was color. This shows that combining three different methods to measure colour, even though adding complexity, was beneficial, and that the ranges picked to quantify scores between 1-10 were good. There was a clear variance between the colour variegation scores for malignant and benign lesions. The feature with the smallest difference was the border irregularity. Irregularity index is a tried and tested method, so the small difference was due to the ranges picked to quantify the scores. This meant that even obviously benign lesions were given a score of 4/5 which is not ideal. This was not a problem for the current project once the total score was found but section 7 recommends solutions to this for future work. The evolution was quantified effectively through the difference in the scores of each

feature over time and the difference in total score which was scaled between 1-10 for clarity. The system responds fast due to steps taken to ensure computational efficiency, which is crucial for a tool that people will use to get results about their health and on a smartphone.

Most importantly, the project provides a result that is simpler to understand than many other papers' results and did not use any complex methods like machine learning that have been difficult for healthcare workers to understand in the past. This project is also valuable in that it allows computers and doctors to work together, while keeping the final decision with the healthcare professional. By bridging the gap between traditional diagnostic methods and cutting-edge technology, the project provided transparent and effective methods to assist in skin cancer detection and is a step forward in the fight against skin cancer. The NHS has realised that there are major risks with black box algorithms, and it has developed technology adoption guidelines that make it necessary for Artificial Intelligence models to be interpretable (Patel, 2023). Having more transparent and interpretable systems like the one from the current project, even though less complex, enhances patient safety since the healthcare workers can understand the computer's process and hence work with it to better diagnose the patient (Patel, 2023). The system's provision of easily interpretable results could contribute to bolstering trust in computer-aided diagnosis among healthcare workers and the general populace.

The system therefore satisfies the objectives of investigating the feasibility of providing a tool that quantifies the ABCDE features of melanoma as well as investigating the motivation for the tool, its design, market, and how it compares to other tools. The results and research proved that the tool is feasible and that there is strong incentive for a project like this.

To further evaluate the proposed tool, a short anonymous online survey was conducted to get a general sense of what people think of this tool (appendices 10a-10b). The survey size was 20 people, 14 not in healthcare and 6 in healthcare. 100% of the people in healthcare said they would use it, mentioning how the system gives reason for its results and how it facilitates rather than replaces healthcare workers' jobs. One healthcare worker mentioned how even though they would use the tool, using histopathological techniques, which involve skin

biopsies, would still be a preferable option for them (appendices 10d-10f). 100% of the non-healthcare respondents were willing to use it. They mentioned how the tool helps when there are obstacles to going to the hospitals like the recent Covid-19 Virus. A former cancer patient mentioned how cancers can indeed be recognized by shape and this tool can help with this. Another respondent mentioned how they would use it but not rely on it (appendices 10g-10j).

However, several issues surfaced during the project. Firstly, the preprocessing and segmentation of the lesions was sometimes not flawless, necessitating manual input from the user. For example, if one image needs more blur in the pre-processing stage than another image, then the user must manually tweak the blur values so that the segmentation can then be accurate. This is problematic because the tool aims to be used by users who are not experts in computer vision and may struggle to comprehend the software code. Secondly, the system has not undergone testing on dark skin toned individuals since the ISIC 2020 dataset comprised mostly of lighter skin tones, which meant the testing was not representative of everyone. Additionally, as was mentioned before, removing the hair from the lesion itself occasionally erased information from the lesion.

7. CONCLUSION AND FURTHER WORK

The current project investigated the motivation for and the feasibility of a tool that quantifies the features of the ABCDE rule of melanoma that can then be used with a physical tool. The methodology involved pre-processing the images to remove unwanted details, segmenting the lesion, and then quantifying the ABCD features between 1-10. Then, weighting was applied to each feature according to their importance to give a total final score out of 24. Then, the evolution was quantified based on the differences in the scores. The results proved that the programme is in fact feasible. The programme can differentiate between benign and malignant moles in terms of their total score, with a few expected exceptions for lesions that had atypical features. The project also proposed a dermatoscope smartphone attachment that can be used with an application of the software. The project involved no machine learning or classification as these can make the system hard to understand. With the current project, healthcare professionals and the general public can be empowered and encouraged to

leverage technology as a valuable aid in melanoma detection, hence facilitating early diagnosis and potentially saving many lives.

The current project could be improved in several ways in the future. Firstly, more images need to be tested, especially people of colour. Secondly, the programme needs to be tested as an application with a smartphone and the dermatoscope attachment to analyse if it works well. Additionally, the ranges picked to quantify border irregularity should be better. There are rarely any benign lesions that had a regularity index of below 1.10 during testing. So, 1.10 and below should give a score of 1, and then go up from there. Furthermore, it would be useful to have an option on the software/app that checks the user's status. This can allow the app to cater specifically to the experience of the person. For instance, if they are healthcare workers, the app can provide data like advanced diagnostic insights and the ability to generate reports for patient records. Moreover, the current project focused on two dimensional images. However, research (Ding et al., 2015) has shown that a combination of two dimensional and three-dimensional imaging can be used to better analyse the lesions. Techniques like photometric stereo can analyse the texture and estimate disruptions to the surface topography of the lesions leading to more accurate assessment of the shape and structure of lesions (Davies and Netlibrary, 2005). Finally, some of the issues with pre-processing and removing hair can be solved via using machine learning methods. (Sabouri, 2016) produced a system that uses Convolutional Neural Networks, a type of neural network in machine learning, to segment images that uses no pre-processing algorithm and hence removes some of the issues with this current project. The current project has made strong contributions and investigated novel approaches, but it would be valuable to try combining both machine learning and the methods investigated through this project. The machine learning could be used only for the tedious aspects, such as pre-processing and removing hair, and should not make any vital decisions. The rest of the programme could remain exactly as it was explained throughout this current project. That way the best aspects of the current project, namely its simplicity and emphasis on human decision making, could remain and the monotonous dull work could be done by machine learning.

Contents for references and appendices

References:	12
Appendix 1:.....	17
Appendix 2:.....	20
Appendix 3:.....	28
Appendix 4:.....	36
Appendix 5:.....	44
Appendix 6:.....	45
Appendix 7:.....	46
Appendix 8:.....	51
Appendix 9:.....	52
Appendix 10:.....	53

References:

- 'DermLite HÜD 2 | Smartphone Home Dermatoscope' (no date) *dermlite.com* [online]. Available from: <https://dermlite.com/products/dermlite-hud-2-home-dermatoscope> [Accessed 16 April 2024].
- 'Geometry and Compactness' (no date) *web.stevenson.edu* [online]. Available from: <https://web.stevenson.edu/mbranson/m4tp/version/1/gerrymandering-math-topic-compactness.html> [Accessed 16 April 2024].
- 'Melanoma skin cancer incidence statistics' (2015) *Cancer Research UK*. 15 May 2015 [online]. Available from: <https://www.cancerresearchuk.org/health-professional/cancer-statistics/statistics-by-cancer-type/melanoma-skin-cancer/incidence#heading-Four> [Accessed 10 October 2023].
- 'Private Skin Cancer Cost | GoPrivate.com' (no date) *www.privatehealth.co.uk* [online]. Available from: <https://www.privatehealth.co.uk/skin-cancer/costs/> [Accessed 15 April 2024].
- 'Signs of Melanoma Skin Cancer | Symptoms of Melanoma' (2023) *www.cancer.org*. 27 October 2023 [online]. Available from: <https://www.cancer.org/cancer/types/melanoma-skin-cancer/detection-diagnosis-staging/signs-and-symptoms.html#:~:text=A%20is%20for%20Asymmetry%3A%20One> [Accessed 16 April 2024].
- 'Skin cancer statistics | World Cancer Research Fund International' (no date) *WCRF International* [online]. Available from: <https://www.wcrf.org/cancer-trends/skin-cancer-statistics/#:~:text=The%20following%20table%20shows%20the%20total%20global%20melanoma> [Accessed 16 April 2024].
- 'THE "ABCDE" RULE' (2016) *Melanoma UK*. 2016 [online]. Available from: <https://www.melanomauk.org.uk/the-abcd-rule> [Accessed 16 April 2024].
- 'The ISIC 2020 Challenge Dataset' (2020) *ISIC 2020 Challenge Dataset*. 2020 [online]. Available from: <https://challenge2020.isic-archive.com/> [Accessed 17 April 2024].
- 'What Does a Pathologist Do and How To Become One? | AUC' (2021) *www.aucmed.edu*. 4 March 2021 [online]. Available from: <https://www.aucmed.edu/about/blog/what-does-a-pathologist-do-and-how-to-become-one#:~:text=A%20pathologist%20studies%20fluid%2C%20tissues> [Accessed 10 October 2023].
- 'Why to use Grayscale Conversion during Image Processing?' (no date) *www.isahit.com* [online]. Available from: <https://www.isahit.com/blog/why-to-use-grayscale-conversion-during-image-processing#:~:text=It%20helps%20in%20simplifying%20algorithms%20and%20as%20well> [Accessed 16 April 2024].
- Agarwal, V. and Patnaik, L. (2021) *Improving Illumination in Night time Images*. 15 March 2021 [online]. Available from: <https://learnopencv.com/improving-illumination-in-night-time-images/> [Accessed 17 April 2024].
- Ali, A.-R., Li, J. and O'Shea, S.J. (2020) Towards the automatic detection of skin lesion shape asymmetry, color variegation and diameter in dermoscopic images. Haass, N.K., ed. *PLOS*

- ONE [online]. 15 (6), p. e0234352. [Accessed 16 April 2024].
- Ali, A.-R.H., Li, J. and Yang, G. (2020) Automating the ABCD Rule for Melanoma Detection: A Survey. *IEEE Access* [online]. 8, pp. 83333–83346.
- Alizadeh, S.M. and Mahloojifar, A. (2018) *A Mobile Application for Early Detection of Melanoma by Image Processing Algorithms IEEE Xplore*. 1 November 2018 [online]. pp. 1–5. Available from: <https://ieeexplore.ieee.org/document/8703575> [Accessed 16 April 2024].
- Ann Pietrangelo (2022) *ABCDE Rule for Skin Cancer: What It Means and How to Use It*. *Healthline*. 10 February 2022 [online]. Available from: <https://www.healthline.com/health/skin-cancer/abcd-rule-for-skin-cancer#how-its-used> [Accessed 16 April 2024].
- baeldung (2023) *Understanding Otsu's Method for Image Segmentation | Baeldung on Computer Science* www.baeldung.com. 23 March 2023 [online]. Available from: <https://www.baeldung.com/cs/otsu-segmentation> [Accessed 16 April 2024].
- Bapat, K. (2018) *Find Center of a Blob (Centroid) Using OpenCV (C++/Python) | Learn OpenCV*. 19 July 2018 [online]. Available from: <https://learnopencv.com/find-center-of/blob-centroid-using-opencv-cpp-python/>.
- Cleveland Clinic (2021) *Melanoma | Cleveland Clinic*. Cleveland Clinic. 21 June 2021 [online]. Available from: <https://my.clevelandclinic.org/health/diseases/14391-melanoma> [Accessed 10 October 2023].
- Curtis, S. (2016) *This £70 gadget lets you test for skin cancer using your smartphone* *The Mirror*. 2 March 2016 [online]. Available from: <https://www.mirror.co.uk/news/technology-science/science/70-gadget-attaches-your-smartphone-7478479> [Accessed 16 April 2024].
- D.J.Dunn (no date) *ENGINEERING COUNCIL CERTIFICATE LEVEL THERMODYNAMIC, FLUID AND PROCESS ENGINEERING C106* [online]. Available from: <http://www.freestudy.co.uk/c106/t1.pdf> [Accessed 16 April 2024].
- Davies, E.R. and Netlibrary, I. (2005) *Machine vision : theory, algorithms, practicalities*. Amsterdam ; Boston, Elsevier.
- Deci Team (2023) *Lesson 3.5: Object Convexity* *Deci*. 11 July 2023 [online]. Available from: <https://deci.ai/course/object-convexity/#:~:text=Defining%20Object%20Convexity> [Accessed 16 April 2024].
- Dermatoscope Comparison*. (no date) [online]. Available from: <https://cdn.bbd.org.uk/uploads/2023/11/19173957/Dermatoscope-Comparison-table.pdf> [Accessed 16 April 2024].
- Ding, Y., John, N.W., Smith, L., Sun, J. and Smith, M. (2015) Combination of 3D skin surface texture features and 2D ABCD features for improved melanoma diagnosis. *Medical & Biological Engineering & Computing* [online]. 53 (10), pp. 961–974. [Accessed 16 April 2024].
- Do, T.-T., Zhou, Y., Zheng, H., Cheung, N.-M. and Koh, D. (2014) *Early Melanoma Diagnosis with Mobile Imaging*. [Accessed 16 April 2024].

- Durgarao, N. and Sudhavani, G. (2018) Detection of Skin Cancer Using ABCD Features. *International Journal of Applied Engineering Research*. 13, pp. 10191–10195. [Accessed 16 April 2024].
- Fernando, S.R. (no date) *Color Detection & Object Tracking Opencv-srf* [online]. Available from: <https://www.opencv-srf.com/2010/09/object-detection-using-color-seperation.html> [Accessed 16 April 2024].
- Firmansyah, H., Kusumaningtyas, E. and Hardiansyah, F. (2017) *Detection Melanoma Cancer using ABCD rule based on Mobile Device*. [Accessed 16 April 2024].
- Garnavi, R., Aldeen, M. and Bailey, J. (2012) Computer-Aided Diagnosis of Melanoma Using Border- and Wavelet-Based Texture Analysis. *IEEE Transactions on Information Technology in Biomedicine* [online]. 16 (6), pp. 1239–1252. [Accessed 16 April 2024].
- GentleCure (2021) *4 Popular Skin Cancer Apps for Early Detection* GentleCure. 22 January 2021 [online]. Available from: <https://www.gentlecure.com/4-popular-skin-cancer-apps-for-early-detection/> [Accessed 16 April 2024].
- Gregory, A. and editor, A.G.H. (15th April 2024) Skin cancer cases reach record high in UK with sharp rise among older adults *The Guardian* [online]. Available from: <https://www.theguardian.com/society/2023/jul/07/skin-cancer-cases-reach-record-high-in-uk-with-sharp-rise-among-older-adults> [Accessed 10 October 2023].
- H.L., S. (2017) *Pixel Intensity Histogram Characteristics: Basics of Image Processing and Machine Vision - Technical Articles* www.allaboutcircuits.com. 7 December 2017 [online]. Available from: <https://www.allaboutcircuits.com/technical-articles/image-histogram-characteristics-machine-learning-image-processing/> [Accessed 16 April 2024].
- Hasler, D. and Suesstrunk, S.E. (2003) Measuring colorfulness in natural images. Rogowitz, B.E. and Pappas, T.N., eds. *SPIE Proceedings* [online]. [Accessed 16 April 2024].
- Jake Ellison (2022) *Many pathologists agree overdiagnosis of skin cancer happens, but don't change diagnosis behavior* UW News. 3 May 2022 [online]. Available from: <https://www.washington.edu/news/2022/05/03/many-pathologists-agree-overdiagnosis-of-skin-cancer-happens-but-dont-change-diagnosis-behavior/> [Accessed 15 April 2024].
- Jovišažunić and Rosin, P. (no date) *A New Convexity Measure for Polygons*. [Accessed 16 April 2024].
- Mahammed, M., Belkaid, A., Cherifi, H., Profile, S., Bessaid, A., Messadi, M. and Bessaid, A. (2014) *Segmentation and ABCD rule extraction for skin tumors classification Segmentation and ABCD rule extraction for skin tumors classification*. [Accessed 16 April 2024].
- Moura, N., Veras, R., Aires, K., Machado, V., Silva, R., Araújo, F. and Claro, M. (2018) ABCD rule and pre-trained CNNs for melanoma diagnosis. *Multimedia Tools and Applications*

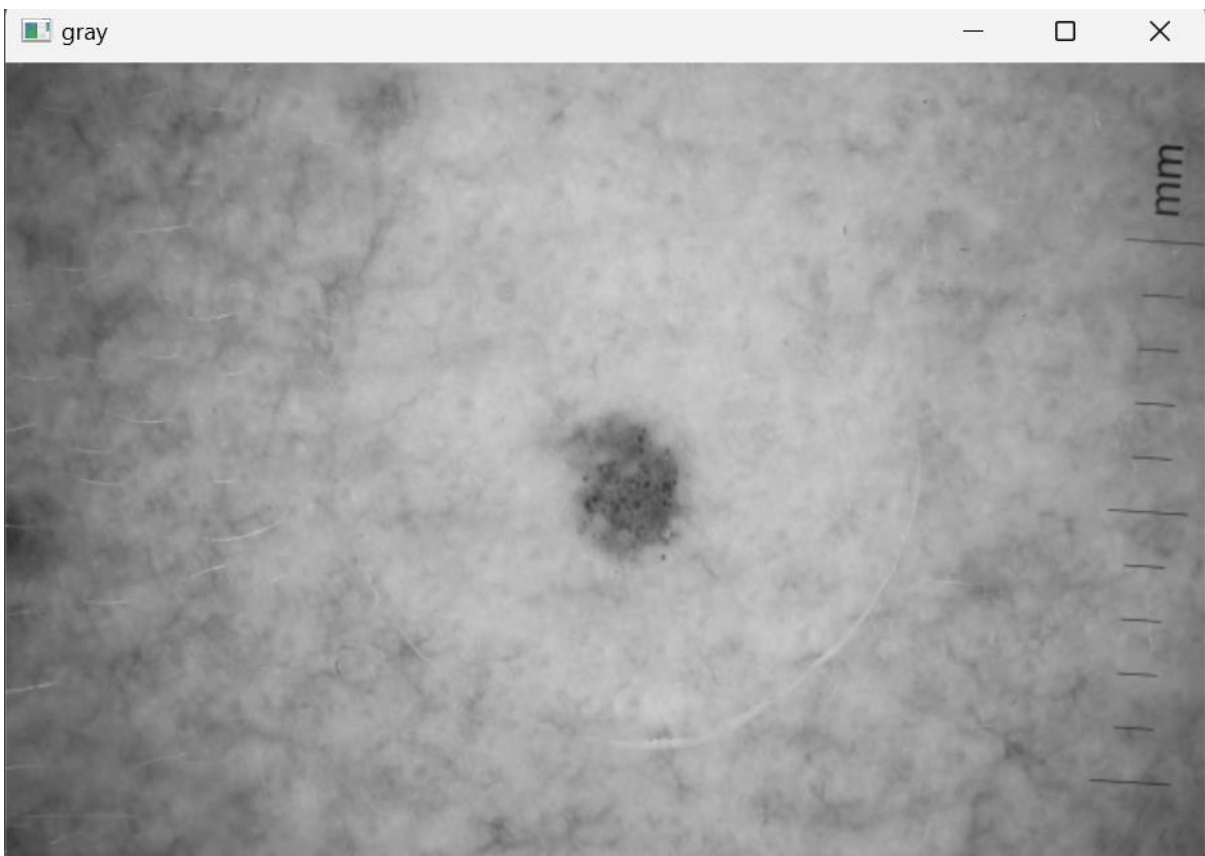
- [online]. 78 (6), pp. 6869–6888. [Accessed 16 April 2024].
- Palus, H. (2006) <title>Colorfulness of the image: definition, computation, and properties</title>. Kolacz, K. and Sochacki, J., eds. *SPIE Proceedings* [online]. [Accessed 16 April 2024].
- Pandey, D. (2021) *Contours and Convex Hull in OpenCV Python Analytics Vidhya*. 19 April 2021 [online]. Available from: <https://medium.com/analytics-vidhya/contours-and-convex-hull-in-opencv-python-d7503f6651bc> [Accessed 16 April 2024].
- Patel, D.A. (2023) *Why lifting the lid on black box AI is essential for healthcare adoption Med-Tech Innovation*. 24 July 2023 [online]. Available from: <https://www.med-technews.com/medtech-insights/ai-in-healthcare-insights/why-lifting-the-lid-on-black-box-ai-is-essential-for-healthc/> [Accessed 16 April 2024].
- Riswanto, U. (2023) *A Beginner's Guide to Image Segmentation using Color Masking Medium*. 20 February 2023 [online]. Available from: <https://ujangriswanto08.medium.com/a-beginners-guide-to-image-segmentation-using-color-masking-3a3fd536ed25> [Accessed 16 April 2024].
- rizvi, M. (2023) *How can I use NumPy to calculate the count of distinct colors in an image? Data Science Dojo Discussions*. 8 May 2023 [online]. Available from: <https://discuss.datasciencedojo.com/t/how-can-i-use-numpy-to-calculate-the-count-of-distinct-colors-in-an-image/1075/2> [Accessed 16 April 2024].
- Rosebrock, A. (2017) *Computing image 'colorfulness' with OpenCV and Python*
- PyImageSearch*. 5 June 2017 [online]. Available from: <https://pyimagesearch.com/2017/06/05/computing-image-colorfulness-with-opencv-and-python/> [Accessed 16 April 2024].
- Sabouri, P. (2016) *Melanoma Detection Using Image Processing and Computer Vision Algorithms Semantic Scholar*. 2016 [online]. Available from: <https://www.semanticscholar.org/paper/Melanoma-Detection-Using-Image-Processing-and-Sabouri/491ca777202343aa5f47a40960ca33249831dd05> [Accessed 16 April 2024].
- She, Z., Liu, Y. and Damatoa, A. (2007) Combination of features from skin pattern and ABCD analysis for lesion classification. *Skin Research and Technology* [online]. 13 (1), pp. 25–33.
- Singh, A. (2019) *SIFT Algorithm | How to Use SIFT for Image Matching in Python (Updated 2023) Analytics Vidhya*. 9 October 2019 [online]. Available from: [https://www.analyticsvidhya.com/blog/2019/10/detailed-guide-powerful-sift-technique-image-matching-python/#:~:text=The%20SIFT%20\(Scale%2DInvariant%20Feature](https://www.analyticsvidhya.com/blog/2019/10/detailed-guide-powerful-sift-technique-image-matching-python/#:~:text=The%20SIFT%20(Scale%2DInvariant%20Feature) [Accessed 16 April 2024].
- Sult, A., Kharusi, A., Keloth, D., Mirza, M., Raj, A., Akkiraju, M., Pillai, B., Ivliev, E. and Obukhov, P. (2021) Comparative analysis of identification of dynamic objects by scale-invariant feature transform and deep neural networks You may also like Investigating the aerodynamic effect of rooftop cargo compartment -a case of modified intercity bus Addis Tefera, Addisu Bekele and Vivek Pandey - Electrically Operated Multipurpose

Trolley Finite Element Method for Predicting the Behavior of Sandwich Structure Luggage Floor of Passenger Cars Comparative analysis of identification of dynamic objects by scale-invariant feature transform and deep neural networks. [online]. [Accessed 16 April 2024].

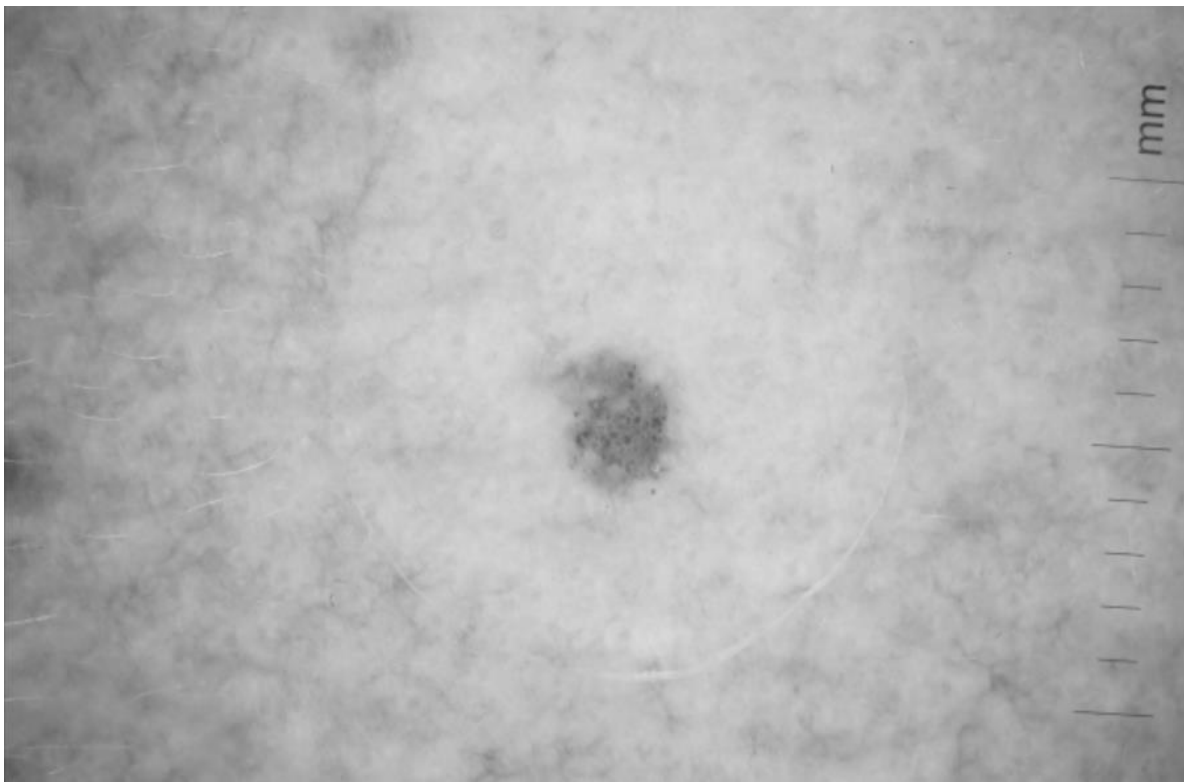
Talavera-Martinez, L., Bibiloni, P. and Gonzalez-Hidalgo, M. (2021) Hair Segmentation and Removal in Dermoscopic Images Using Deep Learning. *IEEE Access* [online]. 9, pp. 2694–2704. [Accessed 16 April 2024].

Velasquez, J. (2022) *Dullrazor algorithm*  GitHub. 10 February 2022 [online]. Available from: <https://github.com/BlueDokk/Dullrazor-algorithm> [Accessed 16 April 2024].

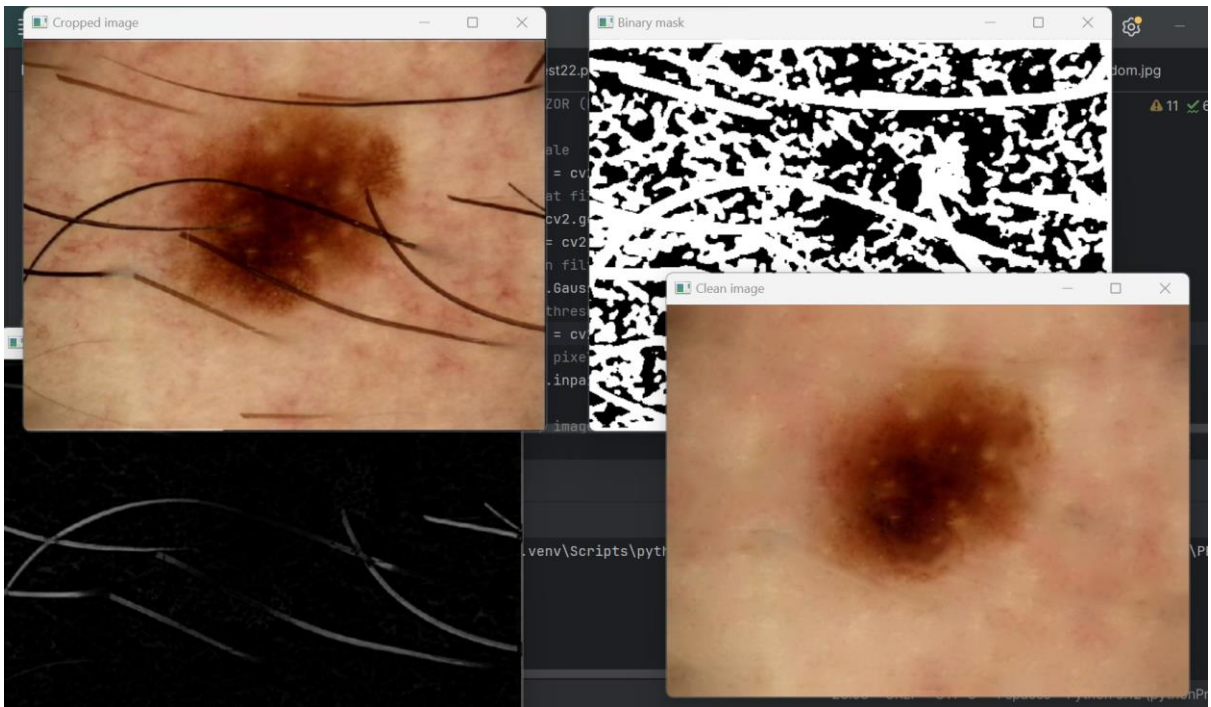
Appendix 1:



Appendix 1a: Gray scale image.



Appendix 1b: Illumination correction applied



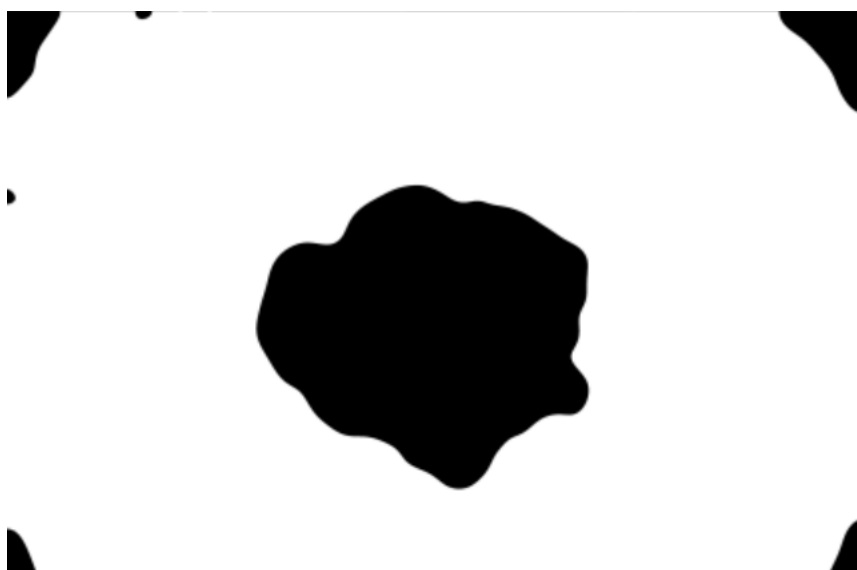
Appendix 1c: An example of successfully removing the hair from a lesion.



Appendix 1d: An example of a lesion where removing the hair removed some essential information, specifically the colour. This was before hair removal.

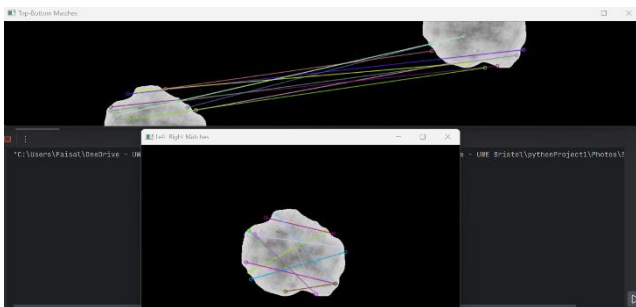


Appendix 1e: An example of a lesion where removing the hair removed some essential information, specifically the colour. This was after hair removal.

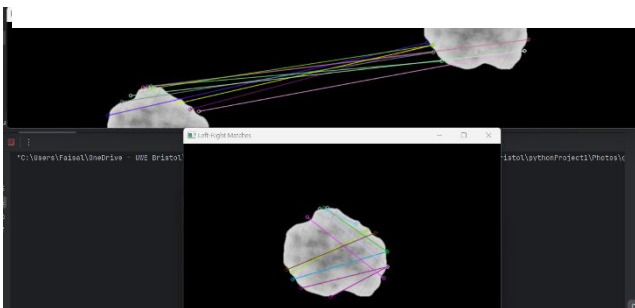


Appendix 1f: Image after thresholding

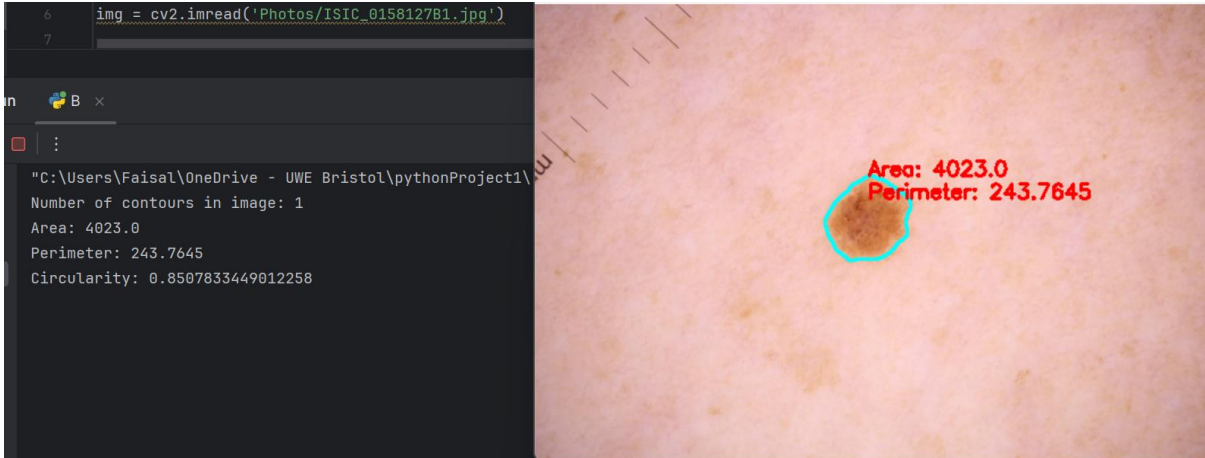
Appendix 2:



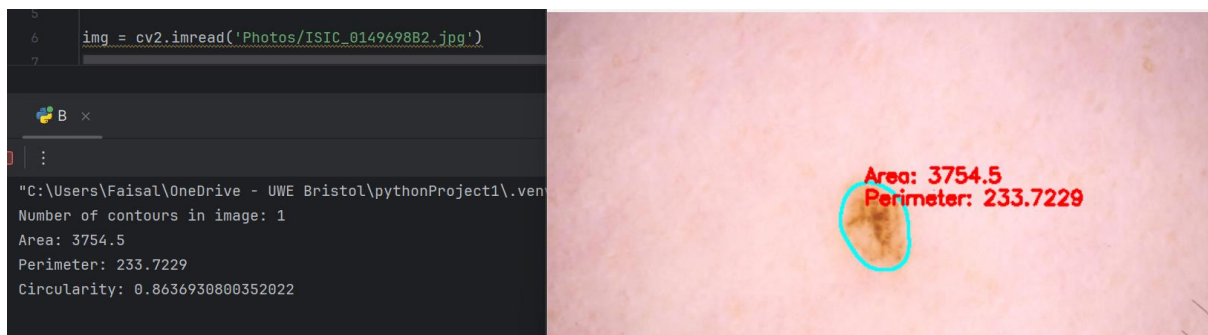
Appendix 2a: SIFT before blurring



Appendix 2b: SIFT after just a little bit of blurring, showing that the matching lines now changed



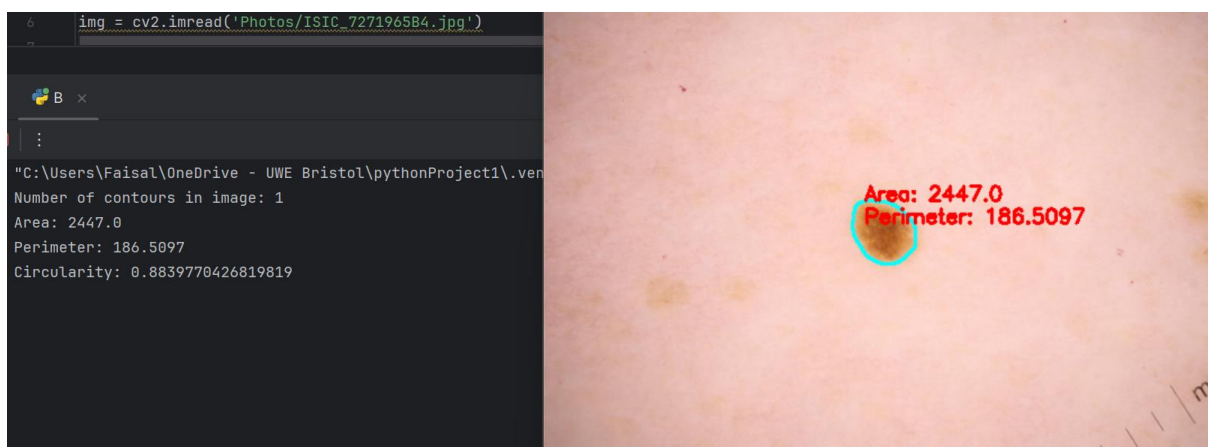
Appendix 2c: Examples of benign lesions tested. Benign lesion 1-circularity calculated



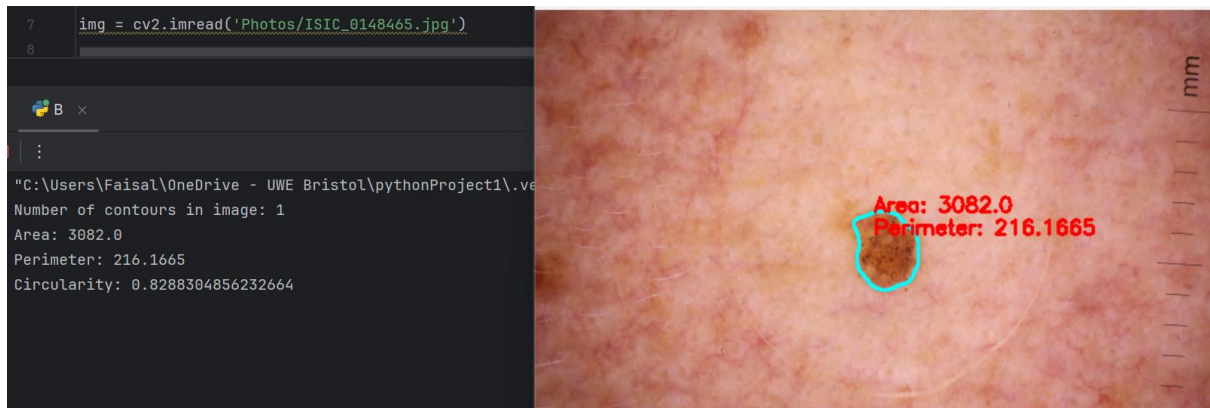
Appendix 2d: Benign lesion 2-circularity calculated



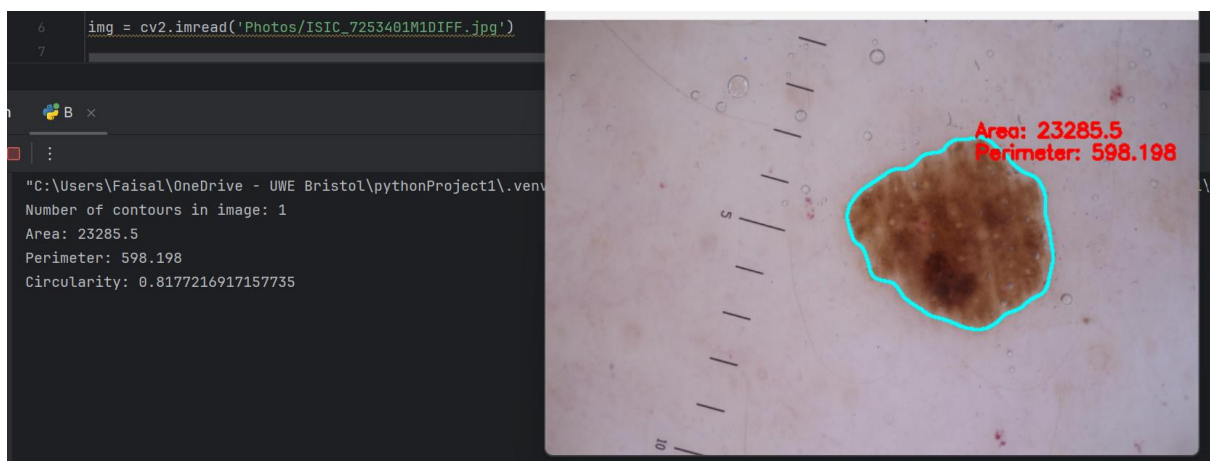
Appendix 2e: Benign lesion 3-circularity calculated



Appendix 2f: Benign lesion 4-circularity calculated



Appendix 2g: Benign lesion 5-circularity calculated



Appendix 2h: Examples of a malignant lesions tested. Malignant lesion 1-circularity calculated



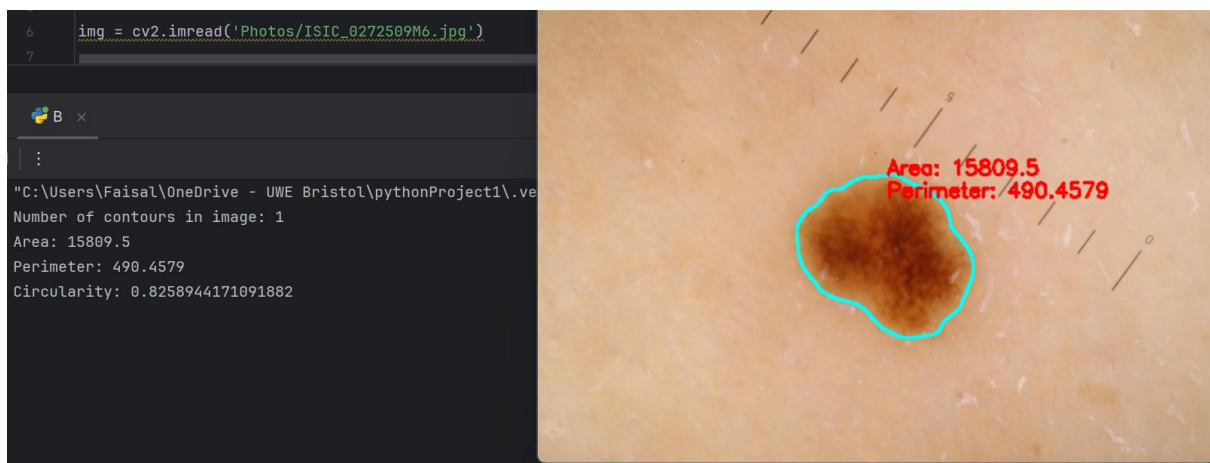
Appendix 2i: Malignant lesion 2-circularity calculated



Appendix 2j: Malignant lesion 3-circularity calculated



Appendix 2k: Malignant lesion 4-circularity calculated



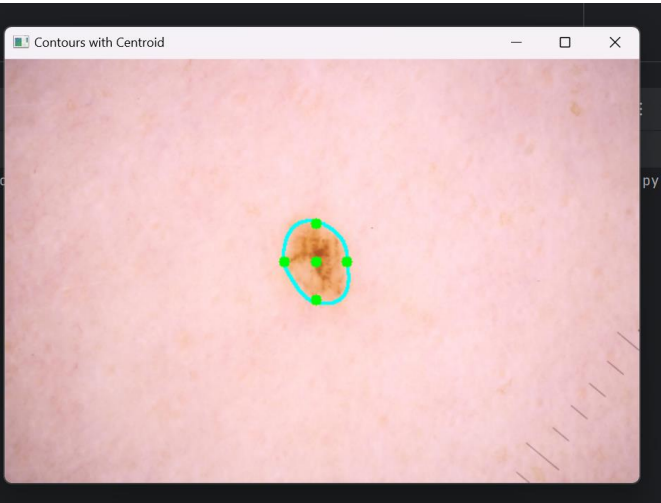
Appendix 2l: Malignant lesion 5-circularity calculated

```
5     img = cv2.imread('Photos/ISIC_0158127B1.jpg')
6
7     for contour in contours > if M["m00"] != 0
8
9         A x
10
11         :
12
13             "C:\Users\Faisal\OneDrive - UWE Bristol\pythonProject1\venv\src\main.py"
14             Centroid Coordinates: 293 188
15             Coordinates Of Top Point: 293 153
16             Coordinates Of Bottom Point : 293 221
17             Coordinates Of Left Point : 256 188
18             Coordinates Of Right Point : 326 188
19             Radius Top: 35
20             Radius Bottom: 33
21             Radius Left: 37
22             Radius Right: 33
23             Difference between top and bottom radius: 2
24             Difference between right and left radius: 4
25             Total difference: 6
```



Appendix 2m: Benign lesion 1-Total difference calculated

```
4
5     img = cv2.imread('Photos/ISIC_0149698B2.jpg')
6     rescaleFrame()
7
8     A x
9
10
11     :
12
13     "C:\Users\Faisal\OneDrive - UWE Bristol\pythonProject1\venv\src\main.py"
14     Centroid Coordinates: 294 191
15     Coordinates Of Top Point: 294 155
16     Coordinates Of Bottom Point : 294 227
17     Coordinates Of Left Point : 264 191
18     Coordinates Of Right Point : 323 191
19     Radius Top: 36
20     Radius Bottom: 36
21     Radius Left: 30
22     Radius Right: 29
23     Difference between top and bottom radius: 0
24     Difference between right and left radius: 1
25     Total difference: 1
```



Appendix 2n: Benign lesion 2-Total difference calculated

```
4
5     img = cv2.imread('Photos/ISIC_0892089B3.jpg')
6
7     for contour in contours > if M["m00"] != 0
8
9         A x
10
11         :
12
13     "C:\Users\Faisal\OneDrive - UWE Bristol\pythonProject1\venv\src\main.py"
14     Centroid Coordinates: 305 178
15     Coordinates Of Top Point: 305 141
16     Coordinates Of Bottom Point : 305 214
17     Coordinates Of Left Point : 267 178
18     Coordinates Of Right Point : 343 178
19     Radius Top: 37
20     Radius Bottom: 36
21     Radius Left: 38
22     Radius Right: 38
23     Difference between top and bottom radius: 1
24     Difference between right and left radius: 0
25     Total difference: 1
```



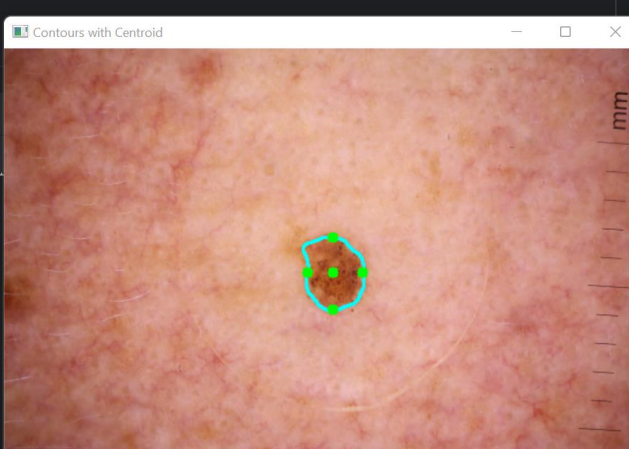
Appendix 2o: Benign lesion 3-Total difference calculated

```
6
7     img = cv2.imread('Photos/ISIC_7271965B4.jpg')
8
for contour in contours : if M["m00"] != 0
Run  A x  B x
5  :
"\"C:\Users\Faisal\OneDrive - UWE Bristol\pythonProject1\.venv\Scripts\python.exe" "C:\Users\Faisal\OneDrive - UWE Bristol\pythonProject1\main.py"
Centroid Coordinates: 301 198
Coordinates Of Top Point: 301 173
Coordinates Of Bottom Point : 301 226
Coordinates Of Left Point : 274 198
Coordinates Of Right Point : 330 198
Radius Top: 25
Radius Bottom: 28
Radius Left: 27
Radius Right: 29
Difference between top and bottom radius: 3
Difference between right and left radius: 2
Total difference: 5
```



Appendix 2p: Benign lesion 4-Total difference calculated

```
>   < Photo 3
>   < Sc 4
>   < sh 5
>   < .gi 6
>   < py 7
for contour in contours : if M["m00"] != 0
Run  A x
5  :
"\"C:\Users\Faisal\OneDrive - UWE Bristol\pythonProject1\.venv\Scripts\python.exe" "C:\Users\Faisal\OneDrive - UWE Bristol\pythonProject1\main.py"
Centroid Coordinates: 310 211
Coordinates Of Top Point: 310 178
Coordinates Of Bottom Point : 310 246
Coordinates Of Left Point : 286 211
Coordinates Of Right Point : 338 211
Radius Top: 33
Radius Bottom: 35
Radius Left: 24
Radius Right: 28
Difference between top and bottom radius: 2
Difference between right and left radius: 4
Total difference: 6
```



Appendix 2q: Benign lesion 5-Total difference calculated

```
4
5     img = cv2.imread('Photos/ISIC_7253401M1DIFF.jpg')
for contour in contours : if M["m00"] != 0
Run  A x
5  :
"\"C:\Users\Faisal\OneDrive - UWE Bristol\pythonProject1\.venv\Scripts\python.exe" "C:\Users\Faisal\OneDrive - UWE Bristol\pythonProject1\main.py"
Centroid Coordinates: 377 195
Coordinates Of Top Point: 377 109
Coordinates Of Bottom Point : 377 280
Coordinates Of Left Point : 278 195
Coordinates Of Right Point : 463 195
Radius Top: 86
Radius Bottom: 85
Radius Left: 99
Radius Right: 86
Difference between top and bottom radius: 1
Difference between right and left radius: 13
Total difference: 14
```



Appendix 2r: Malignant lesion 1-Total difference calculated

The screenshot shows a terminal window with a Python script running. The script reads an image file 'ISIC_0333091MDIFF2.jpg' and performs contour detection and centroid calculation. The output includes various coordinates and radius measurements, followed by a total difference value of 27. To the right of the terminal is a window titled 'Contours with Centroid' displaying a skin lesion with a cyan elliptical contour and three green dots marking the centroid and two other points on the ellipse.

```
4
5     img = cv2.imread('Photos/ISIC_0333091MDIFF2.jpg')
6
Run  A ×
:
"C:\Users\Faisal\OneDrive - UWE Bristol\pythonProject1\.venv\Scripts\python.exe" "C:/Users/Faisal/OneDrive - UWE Bristol/pythonProject1/main.py"
Centroid Coordinates: 297 221
Coordinates Of Top Point: 297 124
Coordinates Of Bottom Point : 297 327
Coordinates Of Left Point : 176 221
Coordinates Of Right Point : 400 221
Radius Top: 97
Radius Bottom: 106
Radius Left: 121
Radius Right: 103
Difference between top and bottom radius: 9
Difference between right and left radius: 18
Total difference: 27
Contours with Centroid
```

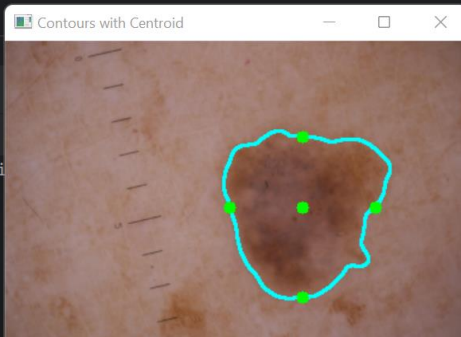
Appendix 2s: Malignant lesion 2-Total difference calculate

The screenshot shows a terminal window with a Python script running. The script reads an image file 'ISIC_0844312MDIFF3.jpg' and performs contour detection and centroid calculation. The output includes various coordinates and radius measurements, followed by a total difference value of 8. To the right of the terminal is a window titled 'Contours with Centroid' displaying a skin lesion with a cyan elliptical contour and three green dots marking the centroid and two other points on the ellipse.

```
5
6     img = cv2.imread('Photos/ISIC_0844312MDIFF3.jpg')
7
8     dcf.detectContours(img)
9
Run  test28 ×
:
Centroid Coordinates: 327 224
Coordinates Of Top Point: 327 147
Coordinates Of Bottom Point : 327 304
Coordinates Of Left Point : 281 224
Coordinates Of Right Point : 378 224
Radius Top: 77
Radius Bottom: 80
Radius Left: 46
Radius Right: 51
Difference between top and bottom radius: 3
Difference between right and left radius: 5
Total difference: 8
Contours with Centroid
```

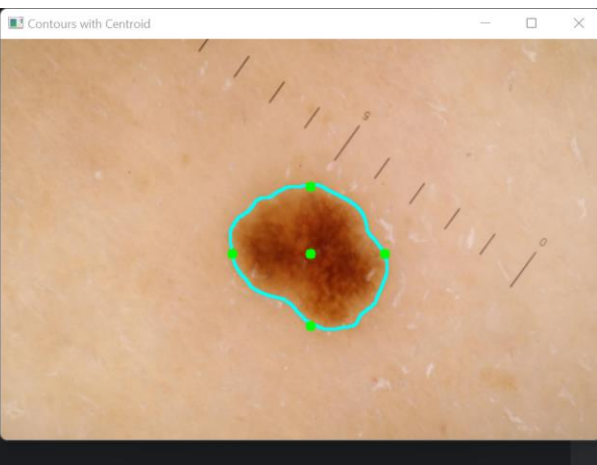
Appendix 2t: Malignant lesion 3-Total difference calculated

```
5     # Load the image
6     img = cv2.imread('Photos/ISIC_1752943M2.jpg')
7
8     for contour in contours : if M['m00'] != 0
9
Run  A ×
:
"C:\Users\Faisal\OneDrive - UWE Bristol\pythonProject1\.venv\Scripts\pyt
Centroid Coordinates: 249 139
Coordinates Of Top Point: 249 80
Coordinates Of Bottom Point : 249 214
Coordinates Of Left Point : 188 139
Coordinates Of Right Point : 310 139
Radius Top: 59
Radius Bottom: 75
Radius Left: 61
Radius Right: 61
Difference between top and bottom radius: 16
Difference between right and left radius: 0
Total difference: 16
```



Appendix 2u: Malignant lesion 4-Total difference calculated

```
4
5     img = cv2.imread('Photos/ISIC_0272509M6.jpg')
6
7     for contour in contours : if M['m00'] != 0
8
Run  A ×
:
"C:\Users\Faisal\OneDrive - UWE Bristol\pythonProject1\.venv\Scripts\pyt
Centroid Coordinates: 309 214
Coordinates Of Top Point: 309 147
Coordinates Of Bottom Point : 309 286
Coordinates Of Left Point : 231 214
Coordinates Of Right Point : 383 214
Radius Top: 67
Radius Bottom: 72
Radius Left: 78
Radius Right: 74
Difference between top and bottom radius: 5
Difference between right and left radius: 4
Total difference: 9
```



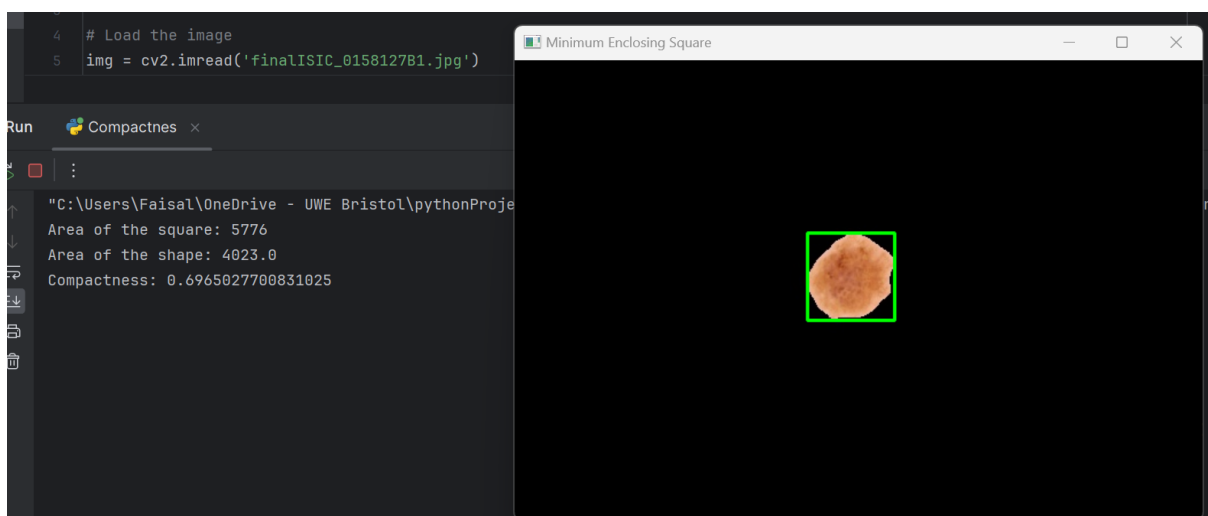
Appendix 2v: Malignant lesion 5-Total difference calculated

Appendix 3:



```
"C:\Users\Faisal\OneDrive - UWE Bristol\pyt  
Convexity ratio: 1.086300803208607
```

Appendix 3a: Convexity ratio measured

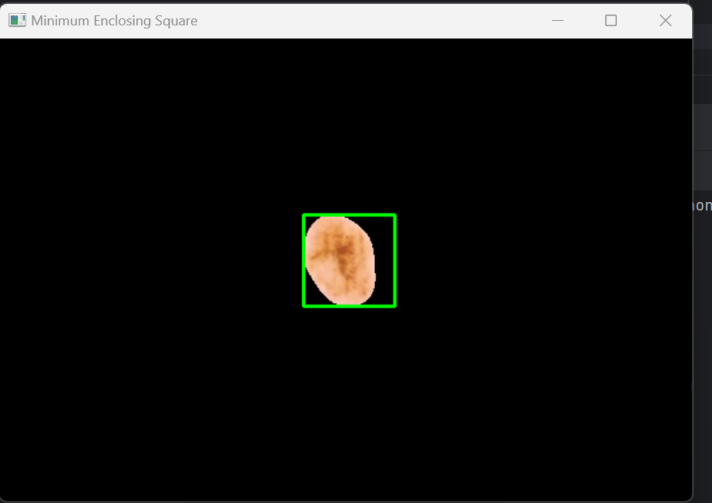


Appendix 3b: Benign lesion 1-compactness measured

```
4 # Load the image
5 img = cv2.imread('finalISIC_0149698B2.jpg')
6

run Compactnes x

C:\Users\Faisal\OneDrive - UWE Bristol\pythonProj
Area of the square: 6241
Area of the shape: 3754.5
Compactness: 0.601586284249319
```

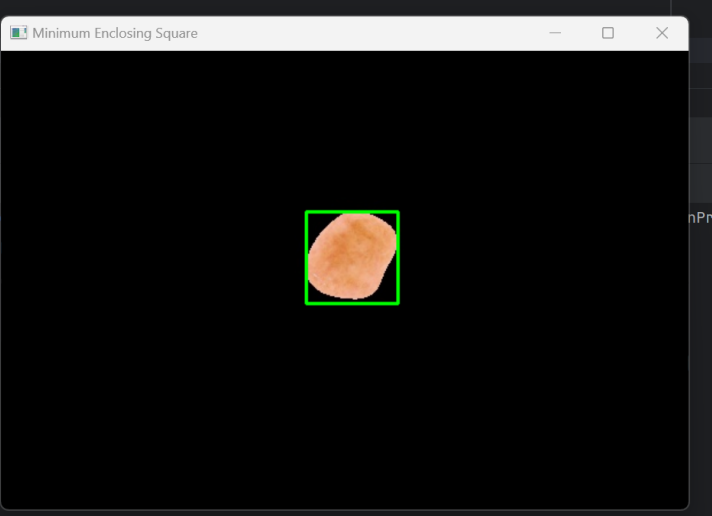


Appendix 3c: Benign lesion 2-compactness measured

```
3
4 # Load the image
5 img = cv2.imread('finalISIC_0892089B3.jpg')
6

run Compactnes x

C:\Users\Faisal\OneDrive - UWE Bristol\pythonProj
Area of the square: 6400
Area of the shape: 4457.5
Compactness: 0.696484375
```



Appendix 3d: Benign lesion 3-compactness measured

The screenshot shows a Python development environment with a dark theme. On the left, a code editor displays the following Python script:

```
4 # Load the image
5 img = cv2.imread('finalISIC_7271965B4.jpg')
6
7 Compactnes x
8
9 : ...
10 "C:\Users\Faisal\OneDrive - UWE Bristol\pythonProject1\
11 Area of the square: 3249
12 Area of the shape: 2447.0
13 Compactness: 0.7531548168667282
```

To the right of the code editor is a window titled "Minimum Enclosing Square" which displays a small, circular brown lesion. A green square frame represents the minimum enclosing square around the lesion.

Appendix 3e: Benign lesion 4-compactness measured

The screenshot shows a Python development environment with a dark theme. On the left, a code editor displays the following Python script:

```
4 # Load the image
5 img = cv2.imread('finalISIC_0148465.jpg')
6
7 Compactnes x
8
9 : ...
10 "C:\Users\Faisal\OneDrive - UWE Bristol\pythonP...
11 Area of the square: 4900
12 Area of the shape: 3082.0
13 Compactness: 0.6289795918367347
```

To the right of the code editor is a window titled "Minimum Enclosing Square" which displays a small, irregular brown lesion. A green square frame represents the minimum enclosing square around the lesion.

Appendix 3f: Benign lesion 5-compactness measured

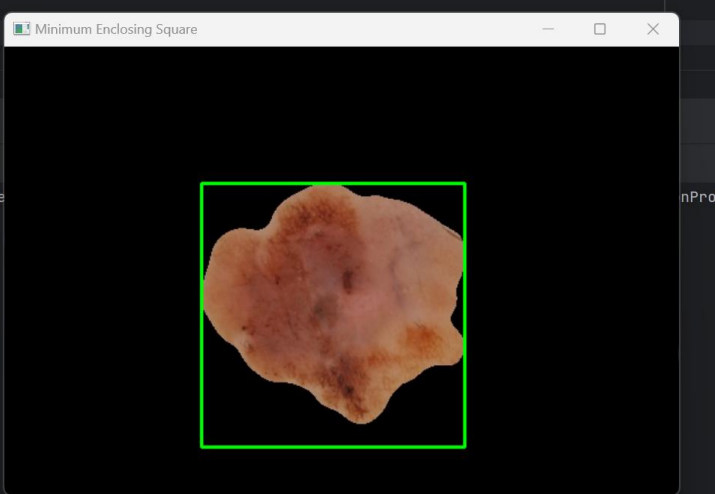
The screenshot shows a Python development environment with a dark theme. On the left, a code editor displays the following Python script:

```
4 # Load the image
5 img = cv2.imread('final7253401M1D1FF.jpg')
6
7 Compactnes x
8
9 : ...
10 "C:\Users\Faisal\OneDrive - UWE Bristol\pythonProject1...
11 Area of the square: 32400
12 Area of the shape: 20504.5
13 Compactness: 0.6328549382716049
```

To the right of the code editor is a window titled "Minimum Enclosing Square" which displays a large, irregular brown lesion. A green square frame represents the minimum enclosing square around the lesion.

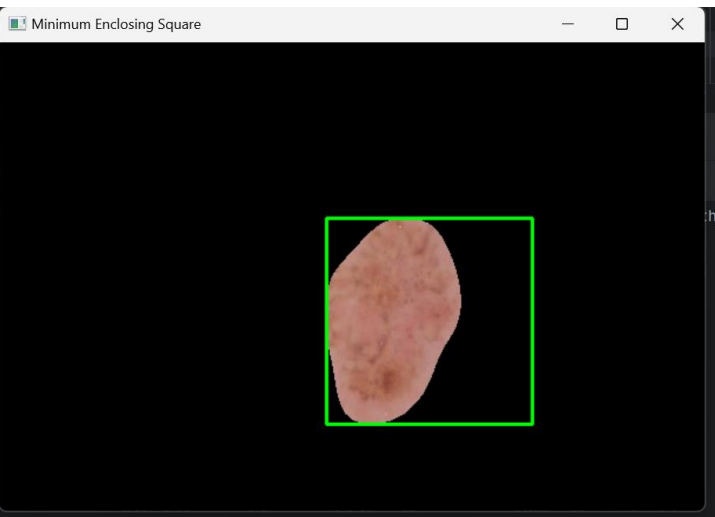
Appendix 3g: Malignant lesion 1-compactness measured

```
4 # Load the image
5 img = cv2.imread('final0333091MDIFF2.jpg')
6
7
8 Compactnes x
9
10
11 "C:\Users\Faisal\OneDrive - UWE Bristol\pythonProject1\final0333091MDIFF2.jpg"
12 Area of the square: 54756
13 Area of the shape: 34477.0
14 Compactness: 0.6296478924684052
```



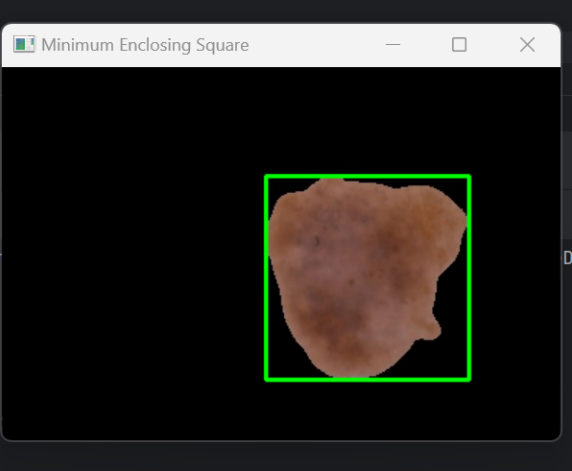
Appendix 3h: Malignant lesion 2-compactness measured

```
4 # Load the image
5 img = cv2.imread('final0844312MDIFF3.jpg')
6
7
8 Compactnes x
9
10
11 "C:\Users\Faisal\OneDrive - UWE Bristol\pythonProject1\final0844312MDIFF3.jpg"
12 Area of the square: 30625
13 Area of the shape: 14870.0
14 Compactness: 0.4855510204081633
```

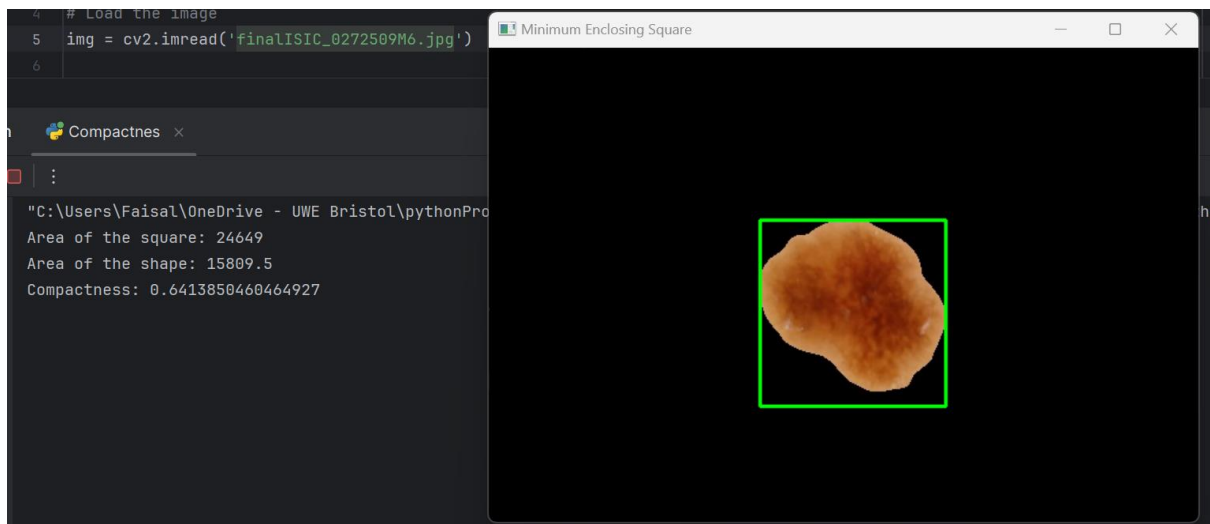


Appendix 3i: Malignant lesion 3-compactness measured

```
4 # Load the image
5 img = cv2.imread('finalISIC_1752943M2.jpg')
6
7
8 Compactnes x
9
10
11 "C:\Users\Faisal\OneDrive - UWE Bristol\pythonProject1\finalISIC_1752943M2.jpg"
12 Area of the square: 19881
13 Area of the shape: 14168.5
14 Compactness: 0.712665358885368
```



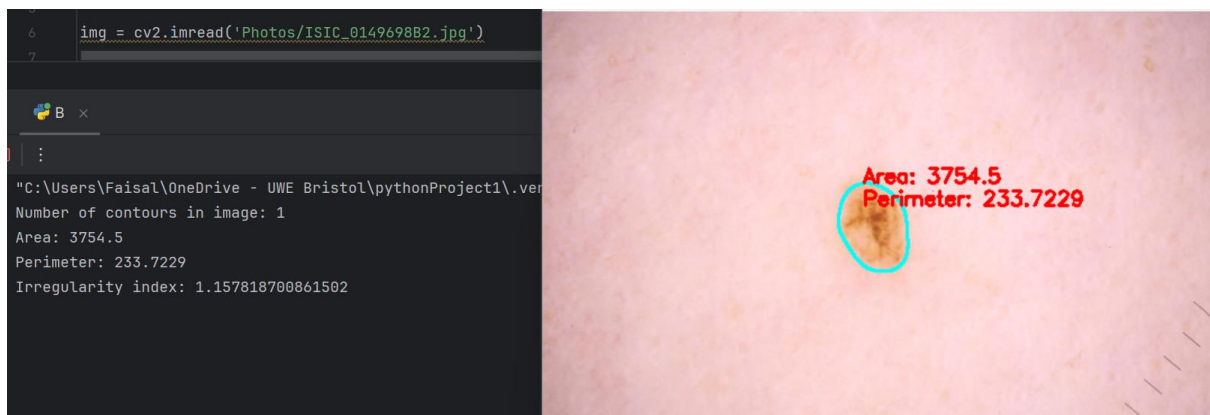
Appendix 3j: Malignant lesion 4-compactness measured



Appendix 3k: Malignant lesion 5-compactness measured



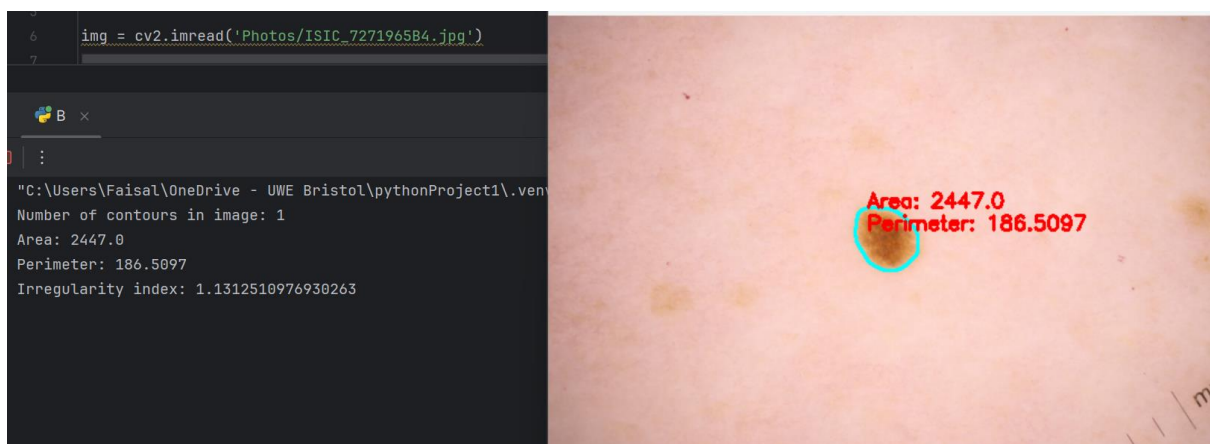
Appendix 3l: Benign lesion 1-irregularity index measured



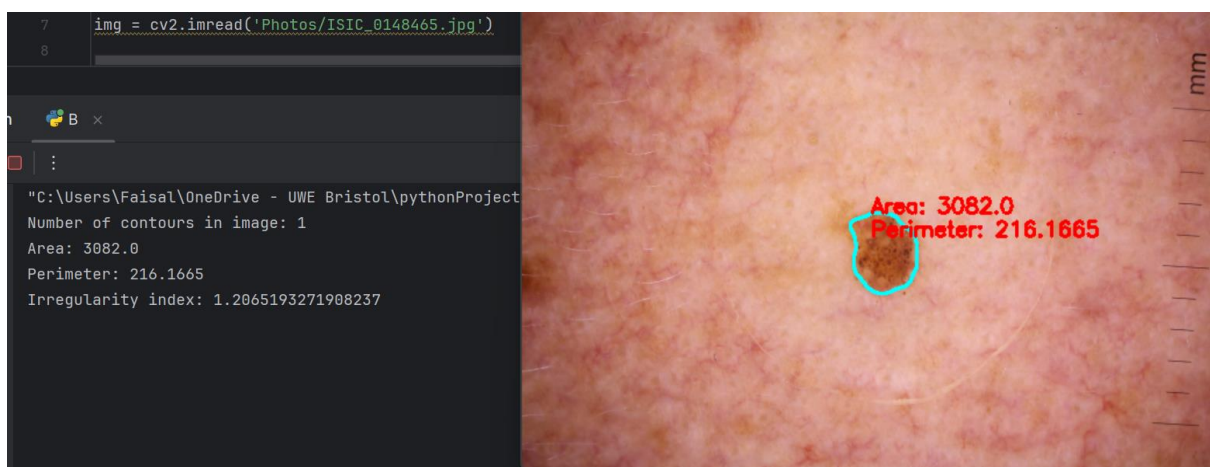
Appendix 3m: Benign lesion 2-irregularity index measured



Appendix 3n: Benign lesion 3-irregularity index measured



Appendix 3o: Benign lesion 4-irregularity index measured



Appendix 3p: Benign lesion 5-irregularity index measured



Appendix 3q: Malignant lesion 1-irregularity index measured



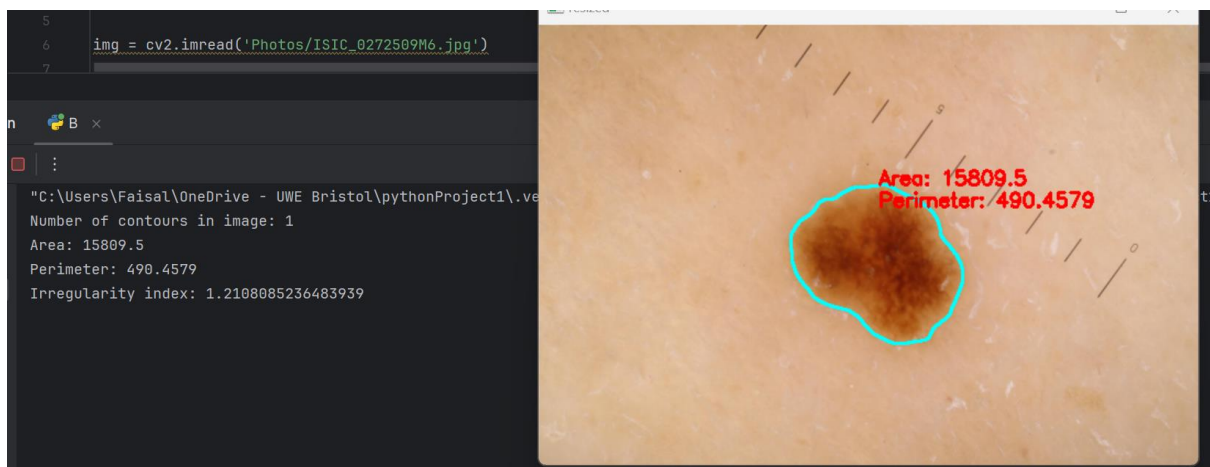
Appendix 3r: Malignant lesion 2-irregularity index measured



Appendix 3s: Malignant lesion 3-irregularity index measured

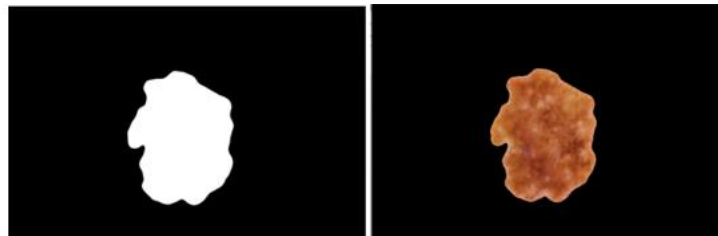


Appendix 3t: Malignant lesion 4-irregularity index measured

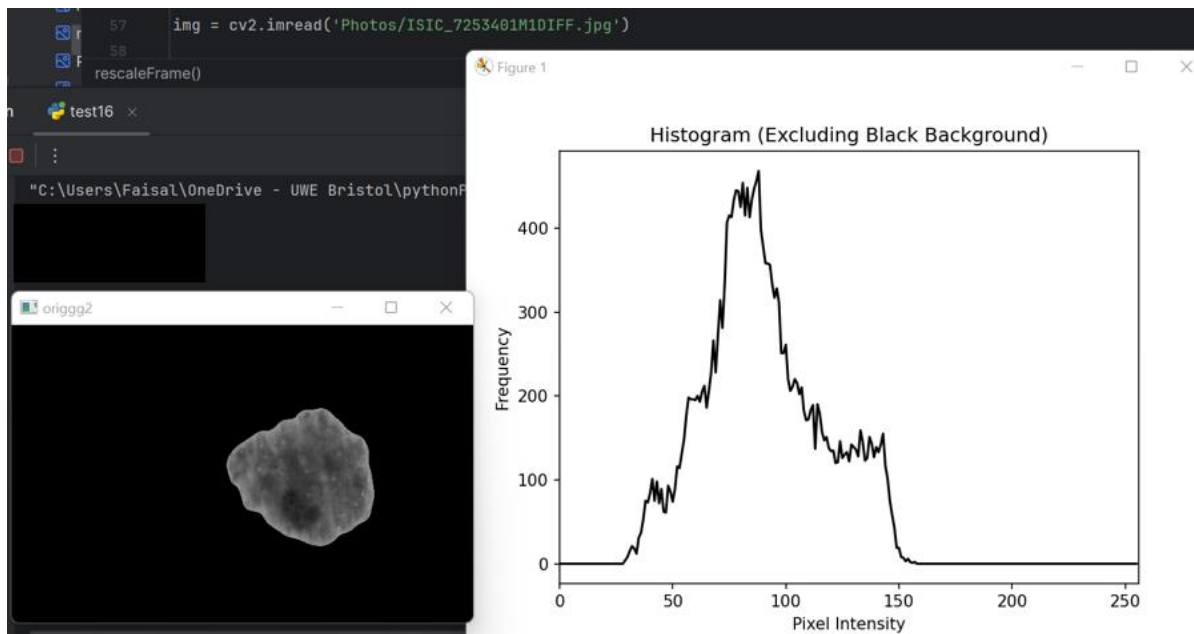


Appendix 3u: Malignant lesion 5-irregularity index measured

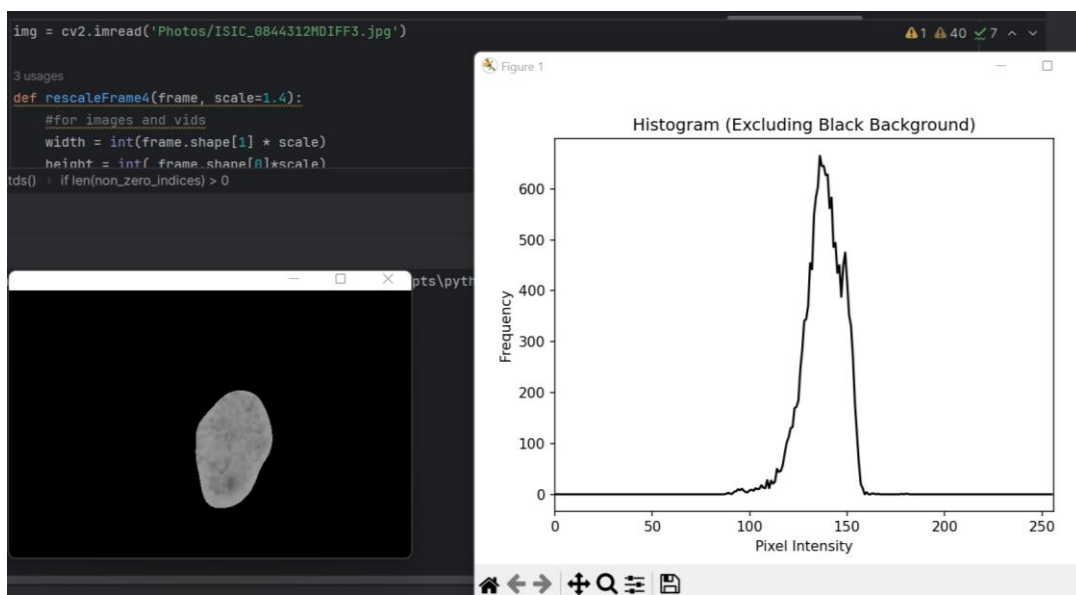
Appendix 4:



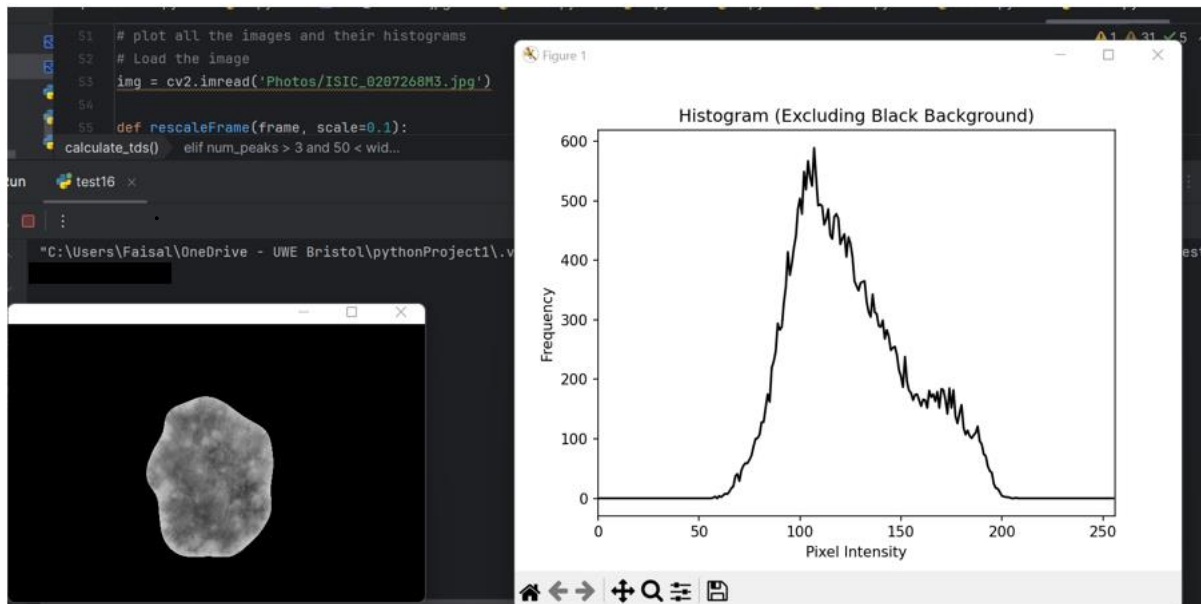
Appendix 4a: before and after imposing the lesion on top of the binary image



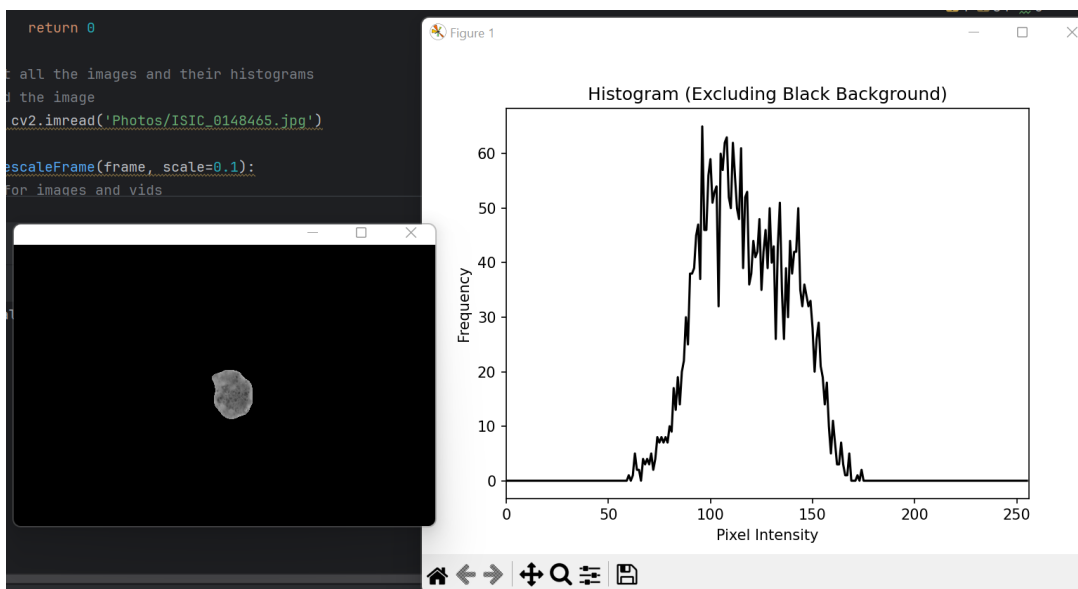
Appendix 4b: Histogram for malignant lesion



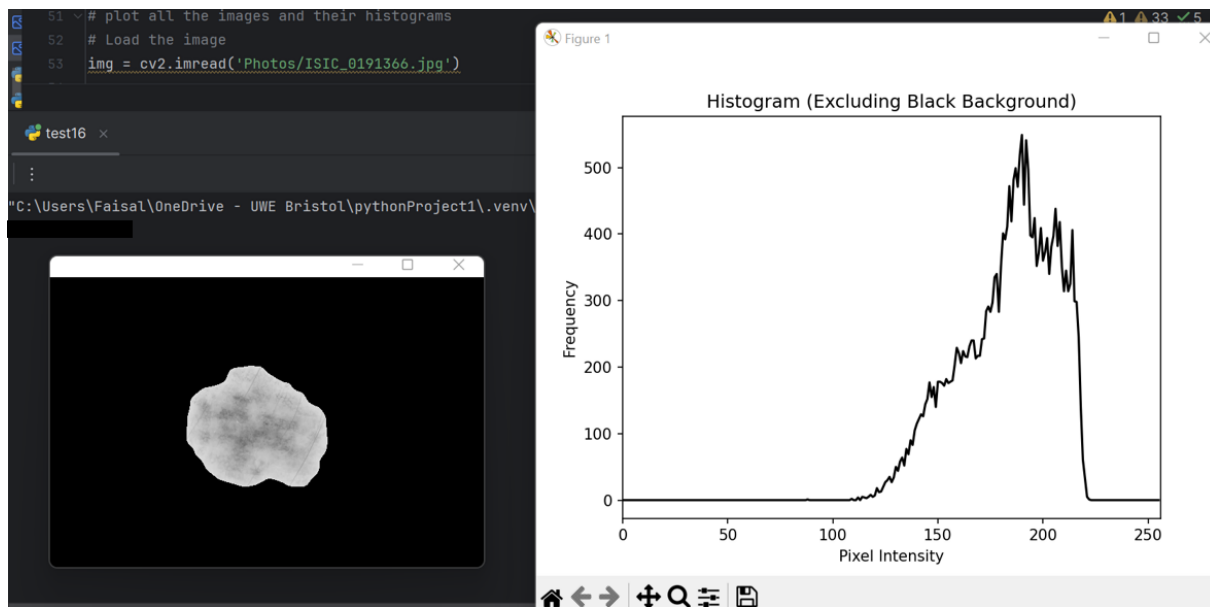
Appendix 4c: Histogram for malignant lesion



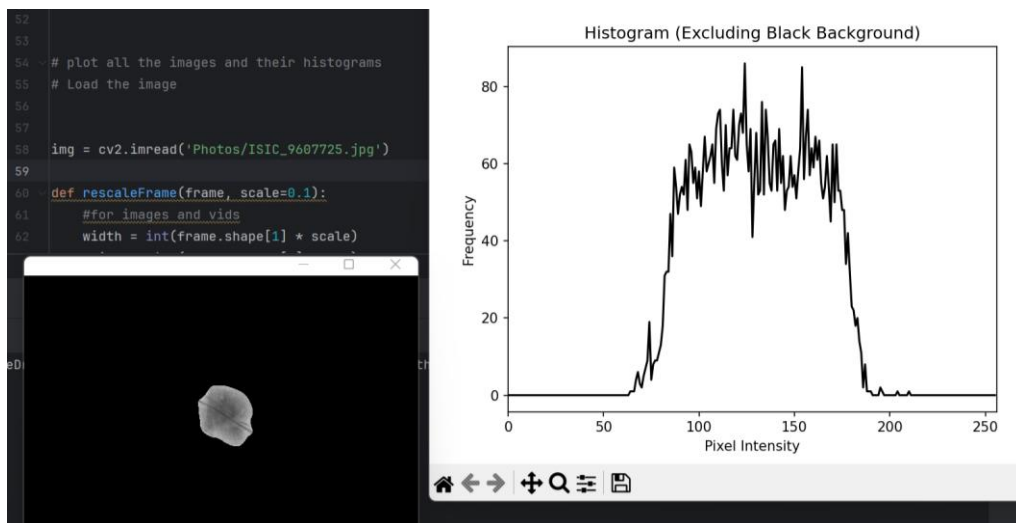
Appendix 4d: Histogram for malignant lesion



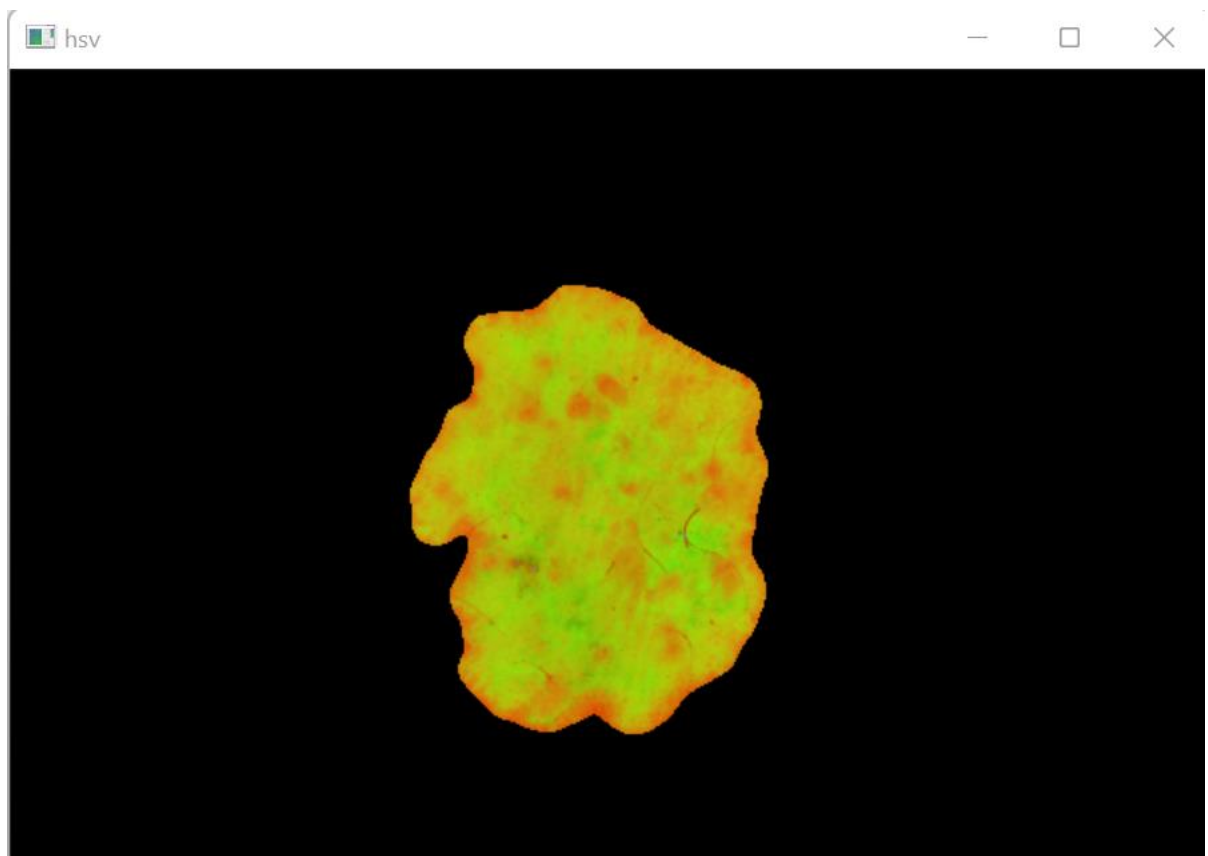
Appendix 4e: Histogram for benign lesion



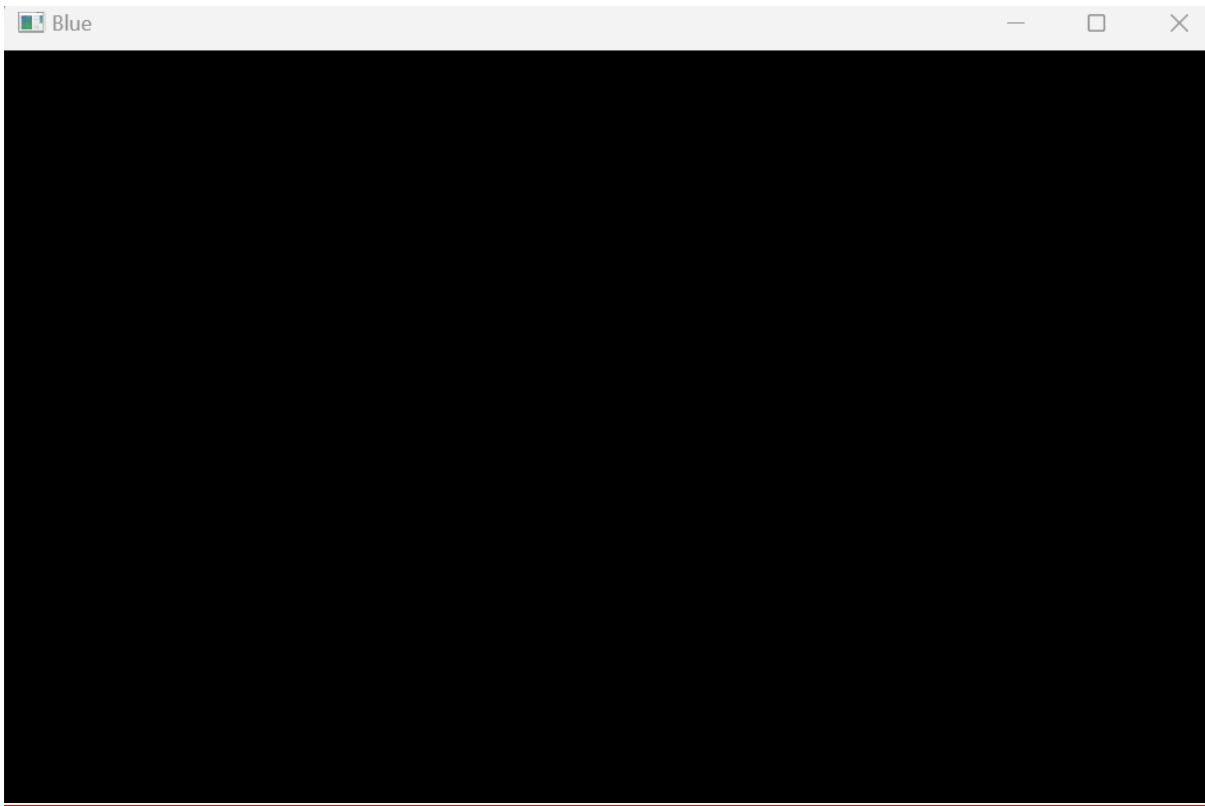
Appendix 4f: Histogram for benign lesion



Appendix 4g: Histogram for benign lesion



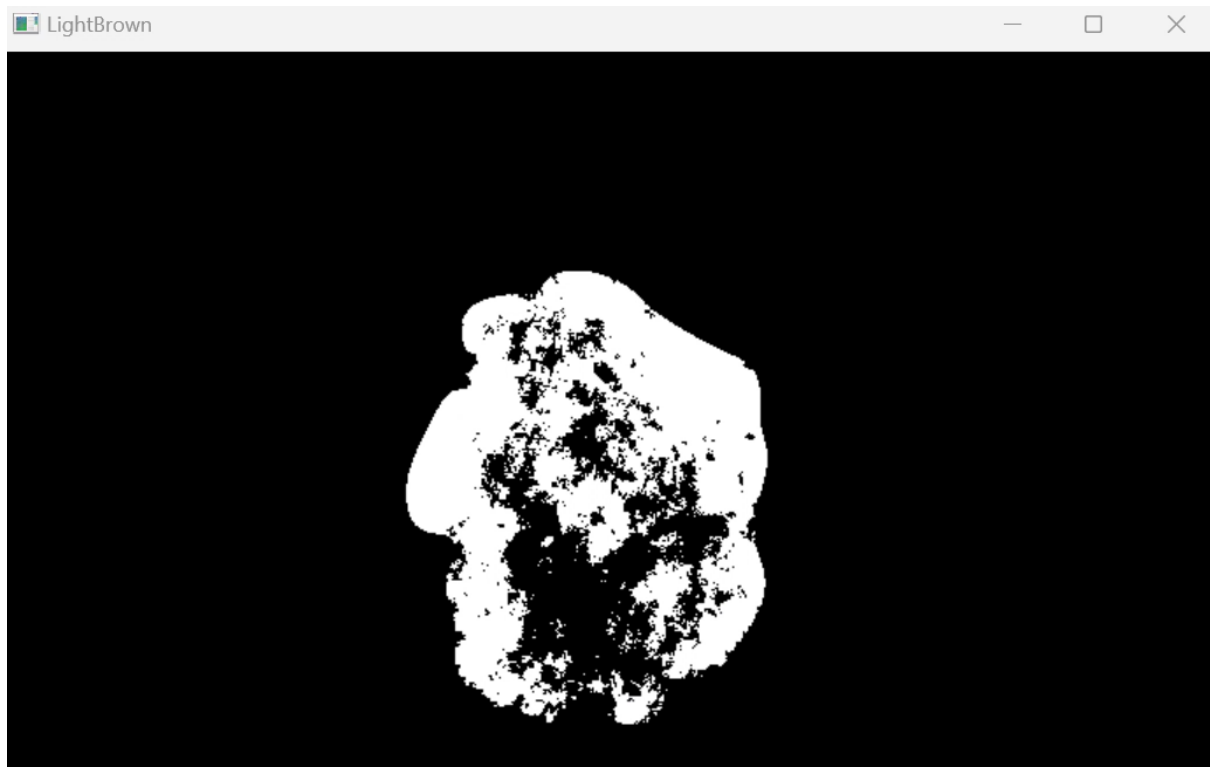
Appendix 4i: Converting lesion to HSV



Appendix 4i: Blue mask-no blue detected



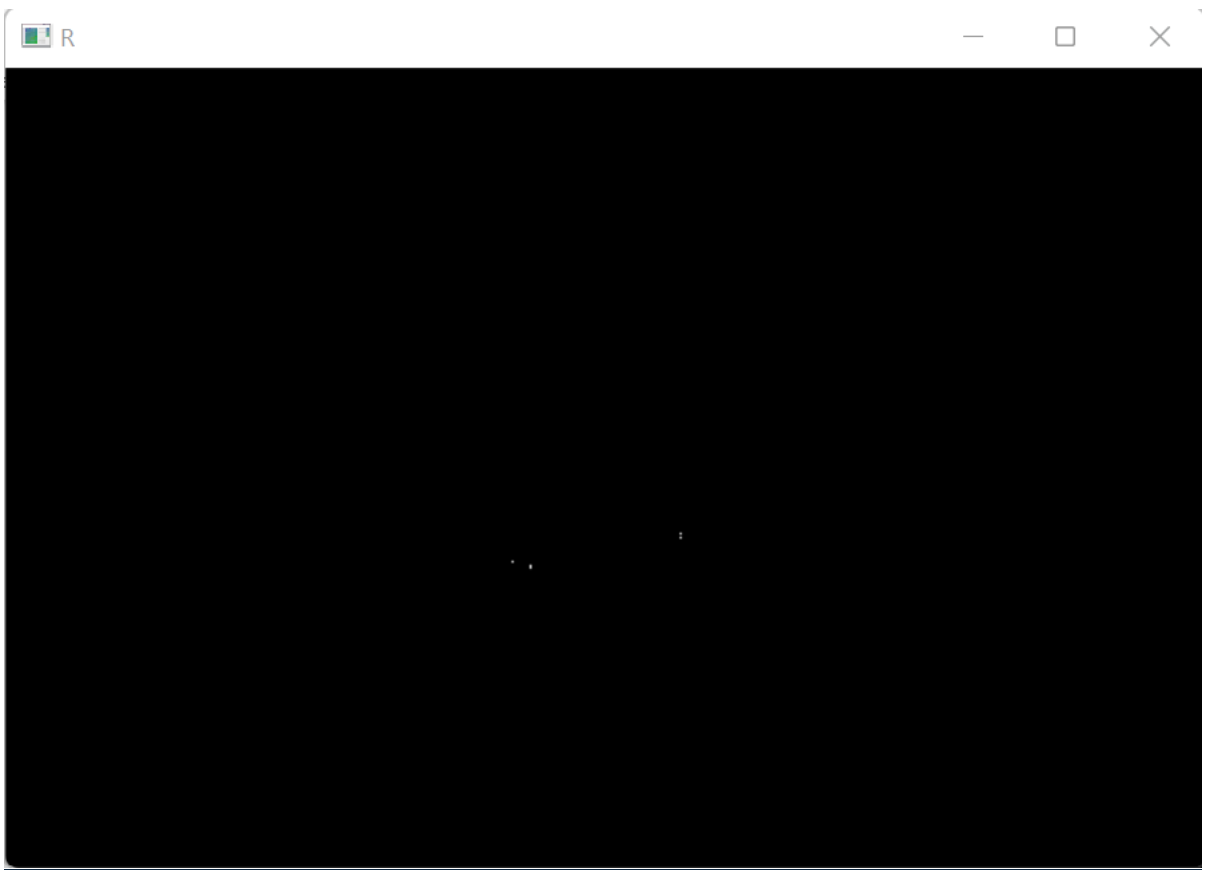
Appendix 4j: Dark brown mask-no colour detected



Appendix 4k: Light brown mask- colour detected



Appendix 4l: White mask-no colour detected



Appendix 4j: Red mask-colour detected

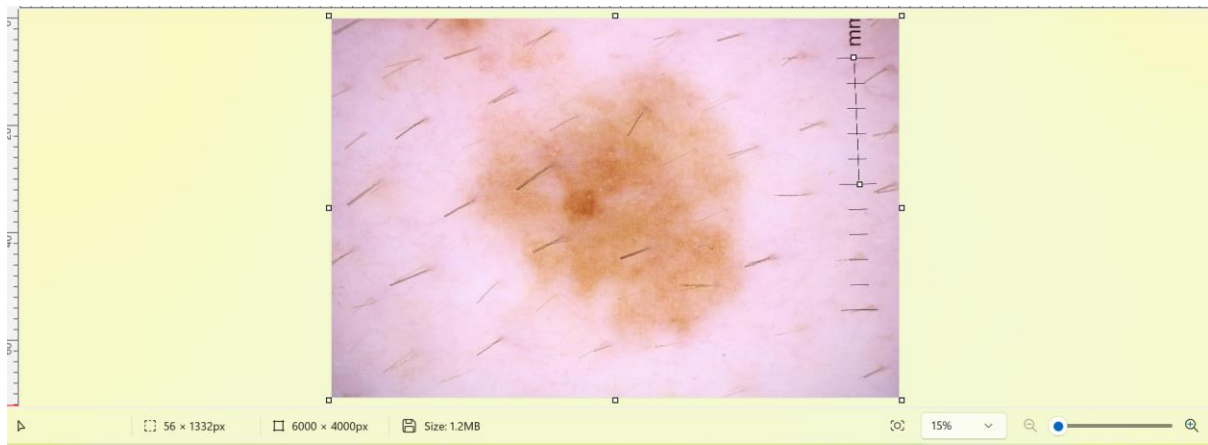


Appendix 4k: Black mask- no colour detected in the lesion, only in the background

```
"C:\Users\Faisal\OneDrive - UWE Bristol\pythonProject1\.  
White: 0  
Dark brown: 0  
Blue: 0  
Black pixel number without mole: 280117  
Black pixel number with mole: 280117  
Black: 0  
Light brown: 1  
Red: 1  
Are you satisfied with the results? (yes/no):
```

Appendix 4l: Results, with option for the specialist to change results if computer made an error

Appendix 5:



Appendix 5a: Using Paint to get the conversion factor

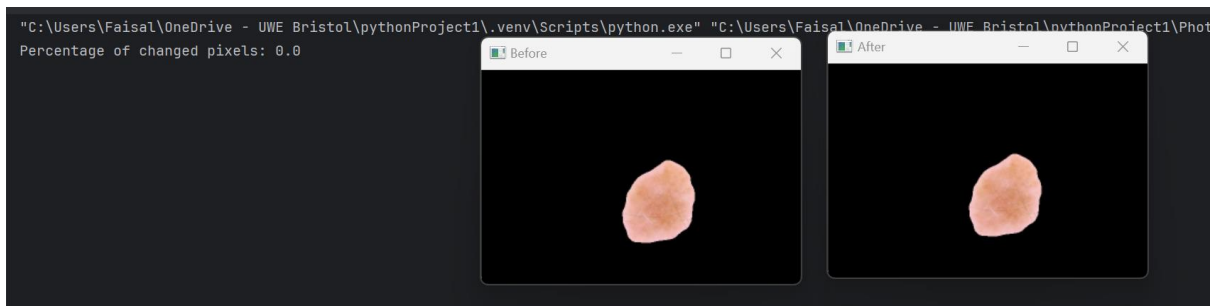
Name of image	Conversion factor (pixels/mm)
ISIC_9998240	263.122
ISIC_0075914	268.120
ISIC_9989641	271.812
ISIC_9750576	272.753
ISIC_9676432	267.067
ISIC_0198375	266.120
ISIC_0351547	267.316
ISIC_9625295	431.419
ISIC_9513918	265.377
ISIC_8889103	266.271
ISIC_9888203	262.195
ISIC_9825222	269.030
ISIC_9906799	433.368
ISIC_0096227	267.187
ISIC_9968669	271.007
ISIC_9987485	269.258
ISIC_9999320	264.486
ISIC_9999127	267.419
ISIC_9978282	265.030
ISIC_9973322	430.116

Total: 5838.473

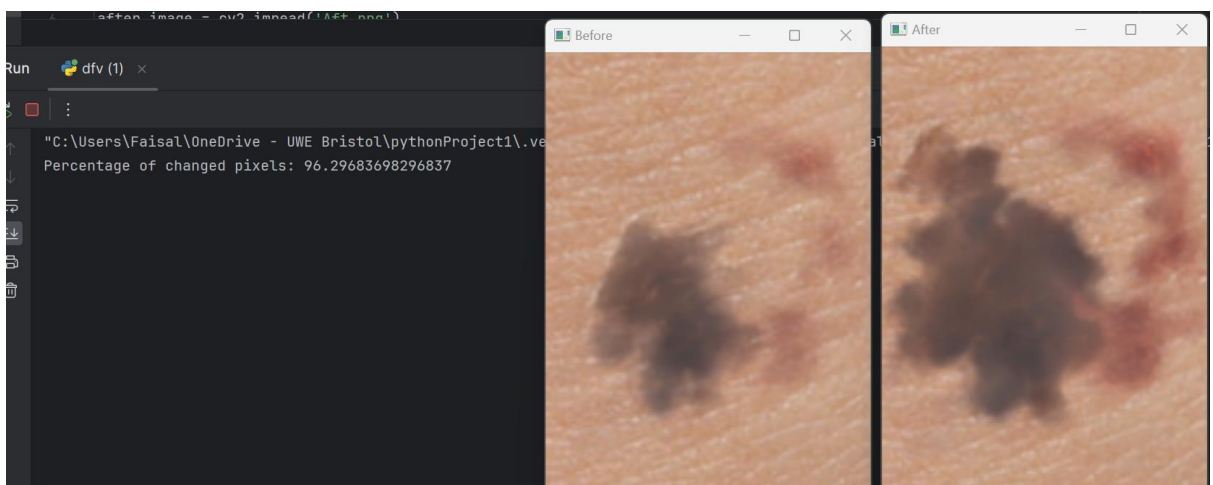
Average: 291.9237

Appendix 5b: Image of the table of twenty images of lesions with dimensions 6000x4000px

Appendix 6:



Appendix 6a: Evolution percentage of skin lesion where no evolution took place.



Appendix 6b: Evolution percetnage of skin lesion where plenty evolution took place.



Appendix 6c: Example of how the evolution of a malignant lesion can be shown on the application.

Appendix 7:



```
8 img = cv2.imread('ISIC_0158127B1.jpg')
9
10 elif 1.2 <= compactness < 1.25
11
12 Run  FinalSystemBenign x
13 | :
14 "C:\Users\Faisal\OneDrive - UWE Bristol\pythonProject"
15 Asymmetry index: 4
16 Border Irregularity Index: 5
17 Colour Variegation Index: 1
18 Diameter Index: 3
19 Total score: 7.7
20 Low risk-less monitoring needed
```

Appendix 7a: Benign lesion final result

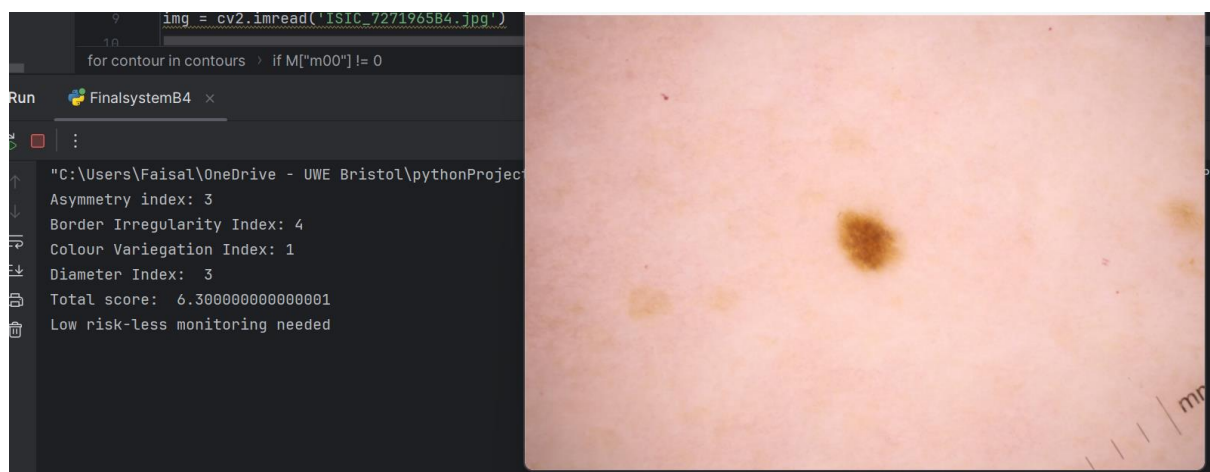


```
8 img = cv2.imread('ISIC_0149698B2.jpg')
9
10 for contour in contours > if M["m00"] != 0
11
12 Run  FinalSystemB2 x
13 | :
14 "C:\Users\Faisal\OneDrive - UWE Bristol\pythonProject"
15 Asymmetry index: 2
16 Border Irregularity Index: 5
17 Colour Variegation Index: 1
18 Diameter Index: 4
19 Total score: 5.6
20 Low risk-less monitoring needed
```

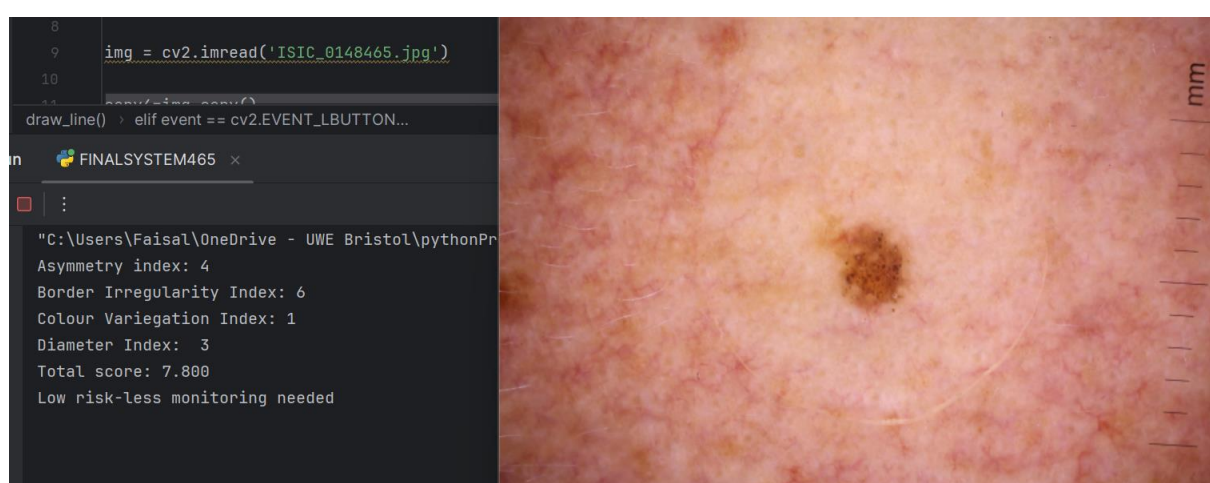
Appendix 7b: Obviously benign lesion final result



Appendix 7c: Obviously benign lesion final result



Appendix 7d: Obviously benign lesion final result



Appendix 7e: Benign lesion final result

```
8     img = cv2.imread('ISIC_0170545B6.jpg')
9
for contour in contours > if M["m00"] != 0
un  finalSystemB6  x
n  :
"C:\Users\Faisal\OneDrive - UWE Bristol\pythonProj
Asymmetry index: 2
Border Irregularity Index: 4
Colour Variegation Index: 1
Diameter Index: 3
Total score: 5.0
Low risk-less monitoring needed

```



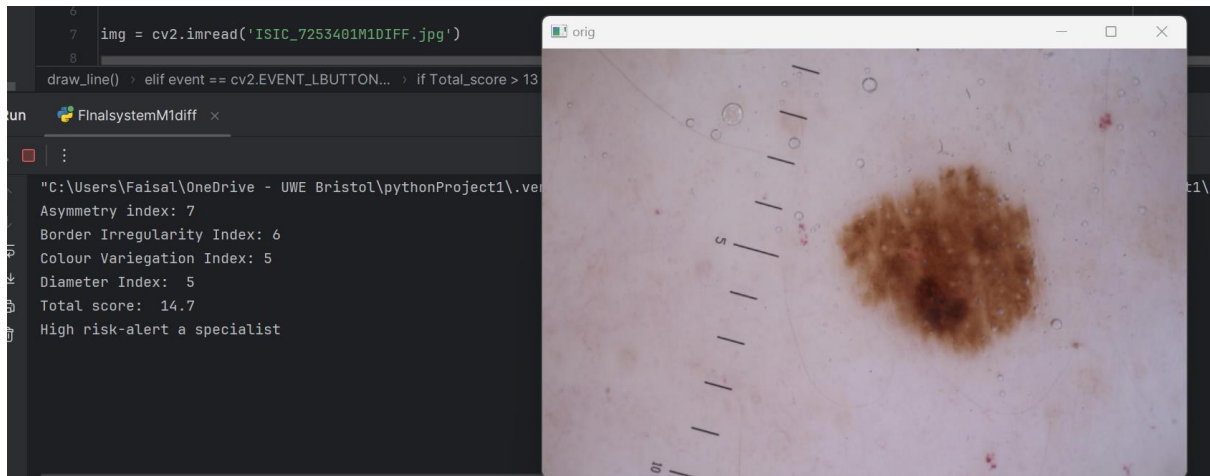
Appendix 7f: Obviously benign lesion final result

```
9     img = cv2.imread('Photos/ISIC_0201689B7.jpg')
10
n  finalSystemB7  x
n  :
"C:\Users\Faisal\OneDrive - UWE Bristol\pythonProject1\
Asymmetry index: 2
Border Irregularity Index: 4
Colour Variegation Index: 1
Diameter Index: 3
Total score: 5.0
Low risk-less monitoring needed

```



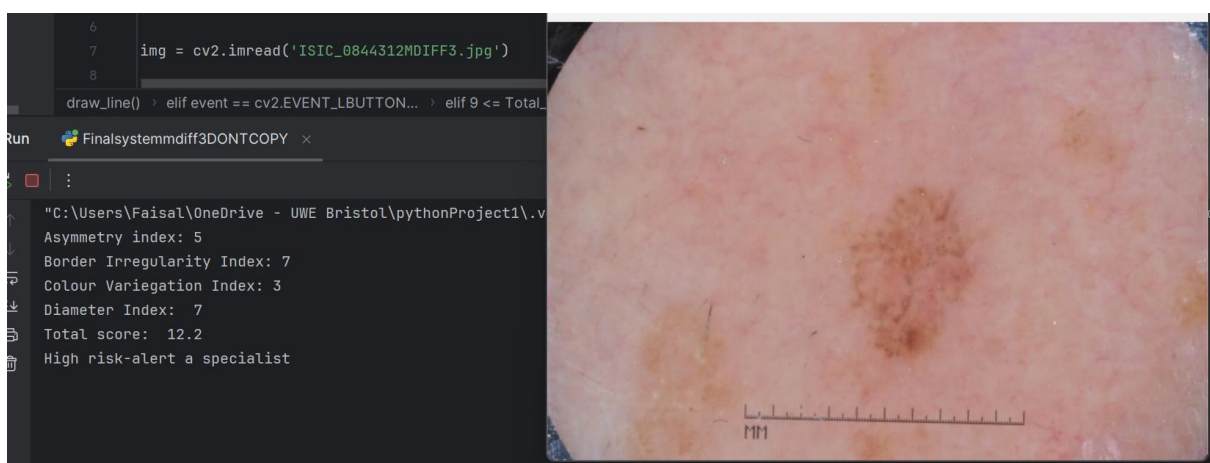
Appendix 7g: Obviously benign lesion final result



Appendix 7i: Obviously malignant lesion final result



Appendix 7j: Obviously malignant lesion final result



Appendix 7k: Malignant lesion final result

```
8 |     img = cv2.imread('ISIC_1752943M2.jpg')
9 |
10| draw_line() > elif event == cv2.EVENT_LBUTTON... > elif 8 < diameter < 9
run  FfinalsystemM2 ×
11| :
12| "C:\Users\Faisal\OneDrive - UWE Bristol\pythonProject1\.venv\...
13| Asymmetry index: 8
14| Border Irregularity Index: 8
15| Colour Variegation Index: 4
16| Diameter Index: 6
17| Total score: 16.2
18| High risk-alert a specialist
```



The screenshot shows a Python code editor with a script named 'finalsystemM2'. The code reads an image file 'ISIC_1752943M2.jpg' and performs a contour analysis. It prints several metrics: Asymmetry index (8), Border Irregularity Index (8), Colour Variegation Index (4), and Diameter Index (6). The total score is calculated as 16.2, which is flagged as a 'High risk-alert a specialist'. To the right of the code is a small window titled 'orig' displaying a skin lesion image with several white lines drawn on it to indicate measurement points.

Appendix 7l: Obviously malignant lesion final result

```
8 | # Load the image
9 | img = cv2.imread('Photos/ISIC_0207268M3.jpg')
10| for i, cnt in enumerate(contour... > if hierarchy[0][i][2] == -1
run  FfinalsystemM3 ×
11| :
12| "C:\Users\Faisal\OneDrive - UWE Bristol\pythonProject1\...
13| Asymmetry index: 6
14| Border Irregularity Index: 5
15| Colour Variegation Index: 10
16| Diameter Index: 10
17| Total score: 18.3
18| High risk-alert a specialist
```



The screenshot shows a Python code editor with a script named 'finalsystemM3'. The code reads an image file 'Photos/ISIC_0207268M3.jpg' and performs a contour analysis. It prints several metrics: Asymmetry index (6), Border Irregularity Index (5), Colour Variegation Index (10), and Diameter Index (10). The total score is calculated as 18.3, which is flagged as a 'High risk-alert a specialist'. To the right of the code is a small window titled 'orig' displaying a skin lesion image with a prominent brownish-orange spot.

Appendix 7n: Obviously malignant lesion final result

```
8 |     img = cv2.imread('ISIC_1785627MDiff5.jpg')
9 |
10| draw_line() > elif event == cv2.EVENT_LBUTTON... > elif diameter > 9
run  Ffinalsystemdiff5 ×
11| :
12| "C:\Users\Faisal\OneDrive - UWE Bristol\pythonProject1\...
13| Asymmetry index: 9
14| Border Irregularity Index: 9
15| Colour Variegation Index: 8
16| Diameter Index: 9
17| Total score: 21.1
18| High risk-alert a specialist
```



The screenshot shows a Python code editor with a script named 'finalsystemdiff5'. The code reads an image file 'ISIC_1785627MDiff5.jpg' and performs a contour analysis. It prints several metrics: Asymmetry index (9), Border Irregularity Index (9), Colour Variegation Index (8), and Diameter Index (9). The total score is calculated as 21.1, which is flagged as a 'High risk-alert a specialist'. To the right of the code is a small window titled 'orig' displaying a skin lesion image with a large brownish-orange area.

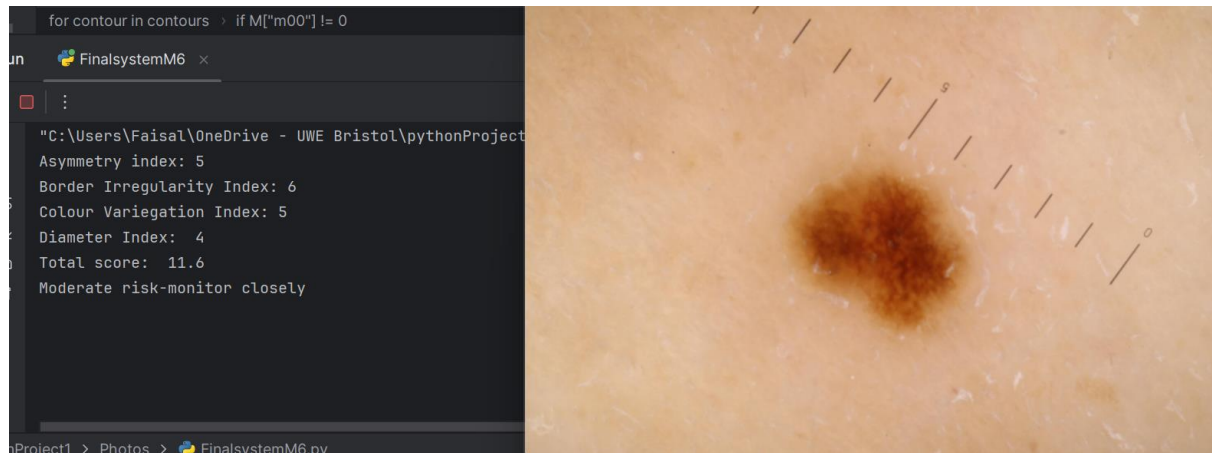
Appendix 7o: Obviously malignant lesion final result

Appendix 8:

The image shows a terminal window and a graphics window side-by-side. The terminal window on the left displays a Python script for image processing and analysis. The script reads an image file named 'ISIC_0341262.jpg' and performs contour detection. It then calculates various metrics for the lesion and outputs a total score and a risk assessment. The graphics window on the right shows a close-up photograph of a skin lesion, which is a dark brown, irregularly shaped spot on light-colored skin.

```
6
7
8     img = cv2.imread('ISIC_0341262.jpg')
9
10    for contour in contours : if M["m00"] != 0
11
12        un  finalsysest 34
13
14        :
15
16        "C:\Users\Faisal\OneDrive - UWE Bristol\python
17        Asymmetry index: 2
18        Border Irregularity Index: 8
19        Colour Variegation Index: 7
20        Diameter Index: 10
21        Total score: 11.9
22        Moderate risk-monitor closely
```

Appendix 8a: Benign lesion outlier



Appendix 8b: Malignant lesion outlier primarily due to small diameter

Appendix 9:

	Benign 1: ISIC_0158127	Benign 2: ISIC_0149698	Benign 3: ISIC_0892089	Benign 4: ISIC_7271965	Benign 5: ISIC_0148465	Benign 6: ISIC_0170545	Benign 7: ISIC_0201689	Benign 8 (outlier): ISIC_0341262	Average
Asymmetry index	4	2	2	3	4	2	2	2	2.625
Border irregularity index	5	5	5	4	6	4	4	8	5.125
Colour variegation index	1	1	1	1	1	1	1	7	1.75
Diameter index	3	4	4	3	3	3	3	10	4.125
	Malignant 1: ISIC_7253401	Malignant 2: ISIC_0333091	Malignant 3: ISIC_0844312	Malignant 4: ISIC_1752943	Malignant 5 (outlier): ISIC_0272509	Malignant 2: ISIC_0207268	Malignant 3: ISIC_1785627	Average	
Asymmetry index	7	10	5	8	5	6	9	7.142857143	
Border irregularity index	6	8	7	8	6	5	9	7	
Colour variegation index	5	9	3	4	5	10	8	6.285714286	
Diameter index	5	10	7	6	4	10	9	7.285714286	
Differences between averages									
Asymmetry index	4.517857143								
Border irregularity index	1.875								
Colour variegation index	4.535714286								
Diameter index	3.160714286								

Appendix 9: Image of the table of the scores for each feature of the 15 images tested, their averages, and the difference between the averages for malignant and benign lesions. Outliers used in calculations for inclusivity.

\

Appendix 10:

Quantifying Melanoma's ABCDE features using computer vision project- Survey

Melanoma is the most dangerous type of skin cancer. Healthcare professionals sometimes may incorrectly diagnose a harmless skin lesion/mole as malignant melanoma, or vice versa. This project proposes a tool that helps with this problem. The tool quantifies, or gives a number from 1-10, to the features of the ABCDE rule that is used to detect Melanoma. The ABCDE rule stands for asymmetry, border irregularity, colour variegation, diameter, and evolution. For example, the first letter of the ABCDE rule stands for asymmetry. The software produced for this tool can look at a picture of a lesion and then measure the asymmetry and then assign a number between 1-10. A score of 10 is very asymmetrical, meaning high risk level, with a score of 1 being the opposite. Weighting is then applied to the numbers. There are other more complex methods (and in some cases more accurate) online that can help with detecting melanoma. These use something called deep learning that classifies the moles as benign or malignant without assigning a numerical score like the tool from this project does. These deep learning methods basically mean the computer makes the decision of whether a lesion is cancerous or not by themselves. This project on the other hand uses simple techniques and aims to help make doctors' jobs easier and more accurate rather than replacing them or doing their job for them. The final decision with this project still lies with the healthcare professional. They simply look at the number assigned for each feature to assist them with their own decisions. Please answer the following questions honestly.

For healthcare professionals only-Would you use a product/programme like this that quantifies the features of melanoma in a clinical setting to help with diagnosing the disease?

Yes

No

Appendix 10a: Part 1 of the survey

For healthcare professionals only-Do you think a programme like the one presented through this project that assigns a numerical score to each skin mole and allows the doctor to make the final decision is better than the second method mentioned that just classified the lesions as malignant or benign that makes the decision itself?

Yes

No

For non healthcare workers only-Would you use a product/programme like this at home through your phone, for example if you suspect you might have melanoma but cannot make the trip to a doctor?

Yes

No

What is your career status?

Healthcare Professional

Other

Please explain your reasons

Create your own automated PDFs with Jotform PDF Editor- [It's free](#)



Appendix 10b: Part 2 of the survey

What is your employment status?

Employed - Healthcare Professional

For healthcare professionals only-Would you use a product/programme like this t...

Yes

For non healthcare workers only-Would you use a product/programme like this at ...

Select an option

For healthcare professionals only-Do you think a programme like the one presente...

Yes

Please explain your reasons

The numerical score would make sense for HCPs due to it actually adding value through giving reason,

The diagnose of melanoma through the appearance of unusual lesions/moles is as important as invasive methods.

Appendix 10c: Healthcare professional response

For healthcare professionals only-Would you use a pr...

Yes

For non healthcare workers only-Would you use a pro...

Select an option

For healthcare professionals only-Do you think a prog...

Yes

Please explain your reasons

Deciding on whether the mole is malignant or benign is preferably using the proper histopathological techniques

Appendix 10d: Healthcare professional response

For healthcare professionals only-Would you use a product/programme like this th...

Yes

For healthcare professionals only-Do you think a programme like the one presente...

Yes

For non healthcare workers only-Would you use a product/programme like this at ...

Select an option

What is your career status?

Healthcare Professional

Please explain your reasons

I think it is a very good concept which removes the risk involved with completely automating the diagnosis process. Instead it facilitates, rather than replaces, the healthcare workers job- a much more trustworthy process for all those involved.

Appendix 10e: Healthcare professional response

For non healthcare workers only-Would you use a product/programme like this at ...

Yes

What is your career status?

Other

Please explain your reasons

it would indicate whether I need to take further action, and take my symptoms more seriously or not

Appendix 10f: Non-healthcare professional response

For non healthcare workers only-Would you use a product/programme like this at ...

Yes

What is your career status?

Other

Please explain your reasons

I would definitely use this at home. It would save me a trip to the hospital specially at the start when there is only a mild suspicion. I believe with this app more people would be educated on the matter. Thus, resulting in more melanomas being diagnosed in early stages.

Appendix 10g: Non- healthcare professional response

For non healthcare workers only-Would you use a product/programme like this at ...

Yes

What is your career status?

Other

Please explain your reasons

Because we don't know what obstacles we faced that prevent us to go to the hospital (like covid-19 virus)

Appendix 10h: Non- healthcare professional response

For non healthcare workers only-Would you use a product/programme like this at ...

Yes

What is your career status?

Other

Please explain your reasons

I believe that the cancer can be recognised by its shape according to my self experience as a patient diagnosed with cancer. Hope this product would help other people for early diagnosis of their health problems.

Appendix 10i: Non- healthcare professional response

For non healthcare workers only-Would you use a product/programme like this at ...

Yes

What is your career status?

Other

Please explain your reasons

If such program was widely trusted in the industry and proved to properly detect signs of melanoma, I would use it as a safety measure/ just to make sure. However, I would not rely on it and would probably regularly check in with a medical professional as well.

Appendix 10j: Non- healthcare professional response